

Dietary methionine influences therapy in mouse cancer models and alters human metabolism

Xia Gao¹, Sydney M. Sanderson^{1,8}, Ziwei Dai^{1,8}, Michael A. Reid¹, Daniel E. Cooper², Min Lu^{3,4}, John P. Richie Jr⁵, Amy Ciccarella⁶, Ana Calcagnotto⁵, Peter G. Mikhael¹, Samantha J. Mentch¹, Juan Liu¹, Gene Ables⁷, David G. Kirsch^{1,2}, David S. Hsu^{3,4}, Sailendra N. Nichenametla⁷ & Jason W. Locasale^{1*}

Nutrition exerts considerable effects on health, and dietary interventions are commonly used to treat diseases of metabolic aetiology. Although cancer has a substantial metabolic component¹, the principles that define whether nutrition may be used to influence outcomes of cancer are unclear². Nevertheless, it is established that targeting metabolic pathways with pharmacological agents or radiation can sometimes lead to controlled therapeutic outcomes. By contrast, whether specific dietary interventions can influence the metabolic pathways that are targeted in standard cancer therapies is not known. Here we show that dietary restriction of the essential amino acid methionine—the reduction of which has anti-ageing and anti-obesogenic properties— influences cancer outcome, through controlled and reproducible changes to one-carbon metabolism. This pathway metabolizes methionine and is the target of a variety of cancer interventions that involve chemotherapy and radiation.

Methionine restriction produced therapeutic responses in two patient-derived xenograft models of chemotherapy-resistant RAS-driven colorectal cancer, and in a mouse model of autochthonous soft-tissue sarcoma driven by a G12D mutation in KRAS and knockout of p53 (*Kras*^{G12D/+}; *Trp53*^{-/-}) that is resistant to radiation. Metabolomics revealed that the therapeutic mechanisms operate via tumour-cell-autonomous effects on flux through one-carbon metabolism that affects redox and nucleotide metabolism—and thus interact with the antimetabolite or radiation intervention. In a controlled and tolerated feeding study in humans, methionine restriction resulted in effects on systemic metabolism that were similar to those obtained in mice. These findings provide evidence that a targeted dietary manipulation can specifically affect tumour-cell metabolism to mediate broad aspects of cancer outcome.

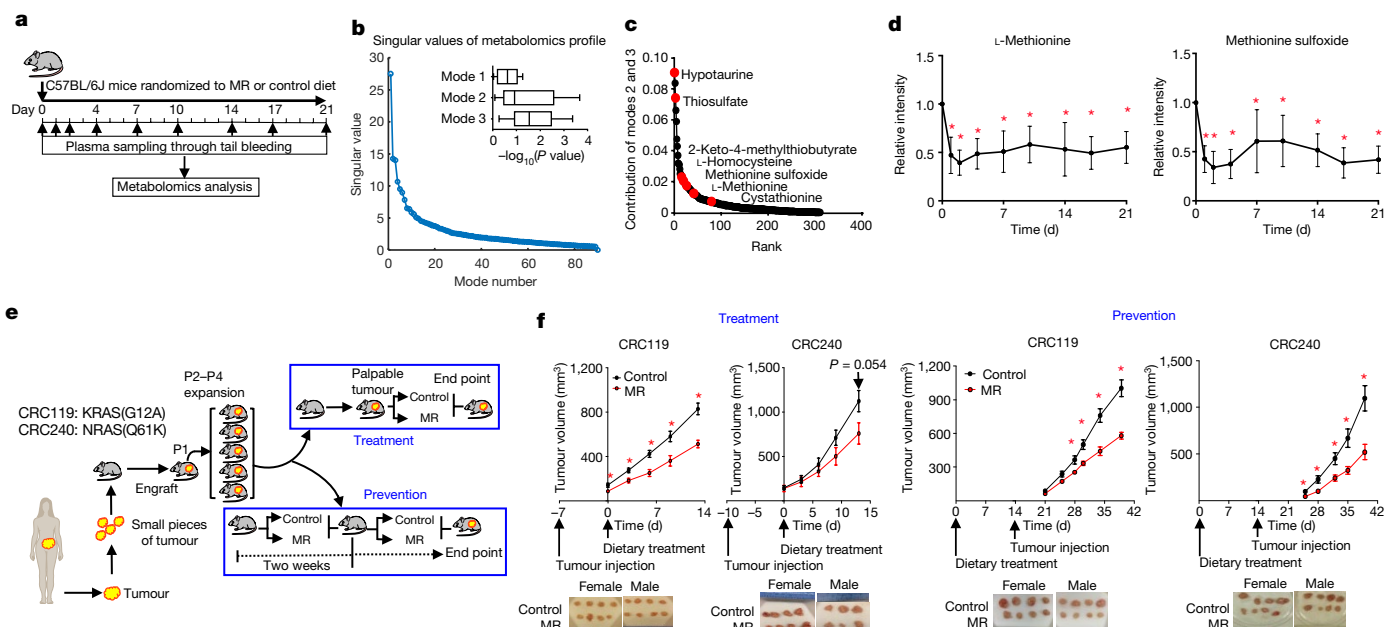


Fig. 1 | Dietary methionine restriction rapidly and specifically alters methionine and sulfur metabolism and inhibits tumour growth in PDX models of colorectal cancer. **a**, Experimental design in C57BL/6J mice. $n = 5$ mice per group. MR, methionine restriction. **b**, Ninety sets of metabolic profiles from a were computed for singular values via singular value decomposition. Insert, two-sided t -test P values assessing the difference between control and methionine restriction in the first three modes. For definitions of the modes, see ‘Analysis of the time-course metabolomics data’ in Methods. $n = 5$ mice per group. Box limits are the 25th and 75th percentiles, centre lines are median, and the whiskers are the

minimal and maximal values. **c**, Contribution of modes 2 and 3 in b ranked across all measured metabolites. **d**, Relative intensity of methionine and methionine sulfoxide. Mean \pm s.d., $n = 5$ mice per group, $*P < 0.05$ by two-tailed Student’s t -test. **e**, Schematic of experimental design using colorectal PDXs. Treatment, $n = 7$ mice per group (4 female and 3 male). Prevention, $n = 8$ mice per group (4 female and 4 male). P1, passage 1; P2, passage 2; P3, passage 3; P4, passage 4. **f**, Tumour growth curve and images of tumours at the end point from e. Mean \pm s.e.m., $*P < 0.05$ by two-tailed Student’s t -test.

¹Department of Pharmacology and Cancer Biology, Duke University School of Medicine, Durham, NC, USA. ²Department of Radiation Oncology, Duke University Medical Center, Durham, NC, USA.

³Center for Genomics and Computational Biology, Duke University, Durham, NC, USA. ⁴Department of Medical Oncology, Duke University Medical Center, Durham, NC, USA. ⁵Department of Public Health Sciences, Penn State University College of Medicine, Hershey, PA, USA. ⁶Penn State University Clinical Research Center, State College, PA, USA. ⁷Orentreich Foundation for the Advancement of Science, Cold Spring, NY, USA. ⁸These authors contributed equally: Sydney M. Sanderson, Ziwei Dai. *e-mail: Jason.Lucasale@duke.edu

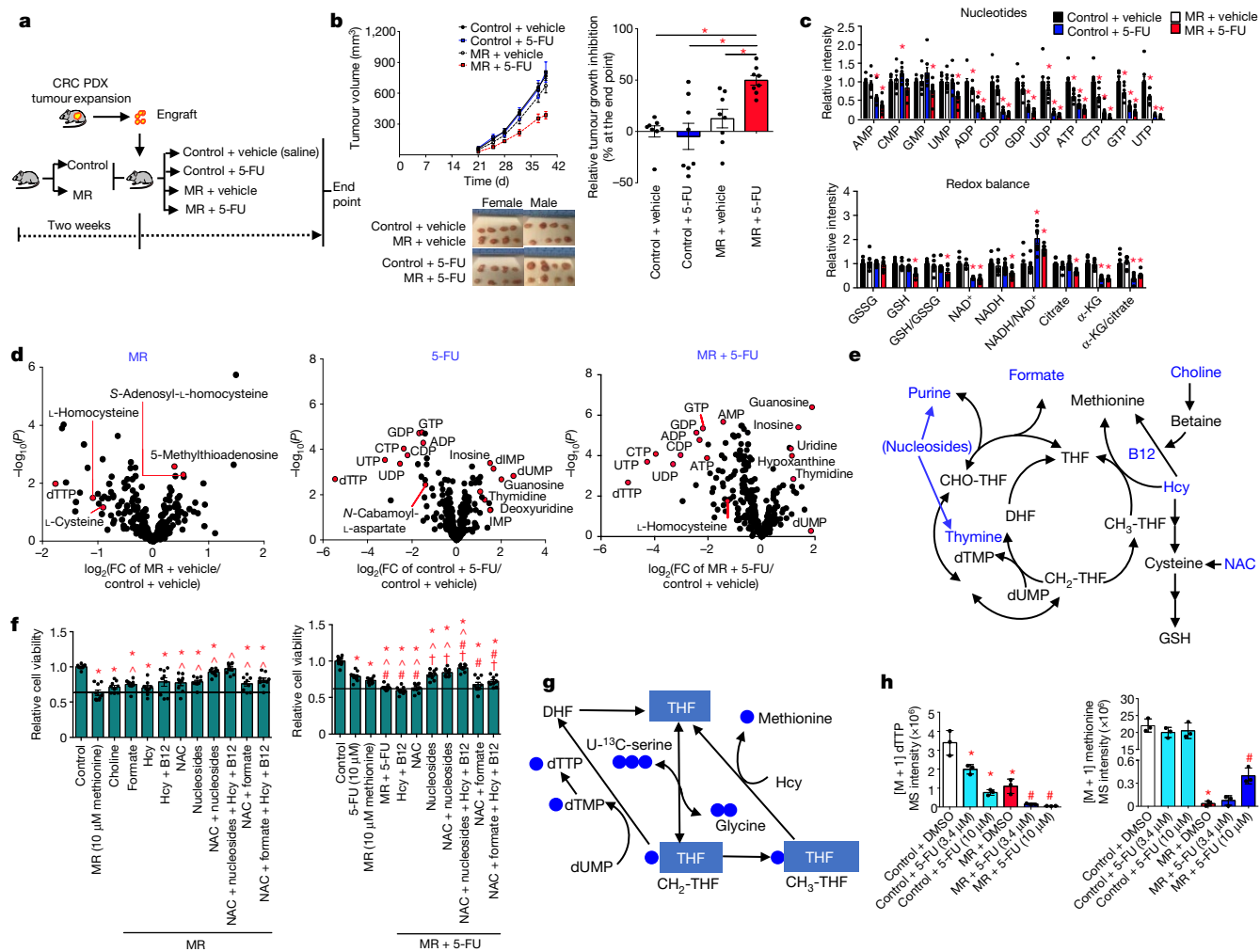


Fig. 2 | Dietary methionine restriction sensitizes PDX models of colorectal cancer to chemotherapy with 5-FU. **a**, Experimental design. CRC, colorectal cancer. **b**, Tumour growth curves, quantification and images at the end point. Mean \pm s.e.m., * P $<$ 0.05 by two-tailed Student's *t*-test. n = 8 mice per group (4 female and 4 male). **c**, Relative intensity of metabolites related to nucleotide metabolism and redox balance in tumours. Mean \pm s.e.m., * P $<$ 0.05 versus control by two-tailed Student's *t*-test. n = 8 mice per group. α -KG, α -ketoglutarate; GSH, glutathione; GSSG, the oxidized form of glutathione. **d**, Volcano plots of metabolites in tumours. FC, fold change. P values were determined by two-tailed Student's *t*-test. **e**, Schematic of supplementation experiments, with added

metabolites in blue. B12, vitamin B12; Hcy, homocysteine. **f**, Effect of nutrient supplements on methionine restriction alone or with 5-FU-inhibited cell proliferation in CRC119 primary cells. Mean \pm s.e.m., n = 9 biologically independent samples from three independent experiments. * P $<$ 0.05 versus control, \wedge P $<$ 0.05 versus methionine restriction, # P $<$ 0.05 versus 5-FU; † P $<$ 0.05 versus methionine restriction + 5-FU by two-tailed Student's *t*-test. **g**, U-¹³C-serine tracing. **h**, Mass intensity for [M + 1] dTTP and [M + 1] methionine in CRC119 cells. MS, mass spectra. Mean \pm s.d., n = 3 biologically independent samples. * P $<$ 0.05 versus control, # P $<$ 0.05 versus methionine restriction by two-tailed Student's *t*-test.

Nutrient composition in growth media has marked effects on cancer cell metabolism^{3–5}. However, the extent to which diet—through its influence on levels of circulating metabolites (which is the *in vivo* equivalent of medium nutrient composition)—alters metabolic pathways in tumours and affects therapeutic outcomes is largely unknown. Previous studies have shown that the dietary removal of serine and glycine can modulate cancer outcome^{6–8}. The availability of histidine and asparagine mediates the response to methotrexate⁹ and the progression of breast cancer metastasis¹⁰, respectively. Whether such interventions broadly affect metabolism or have targeted effects on specific pathways related to these nutrients is unknown. One possibility for a specific dietary intervention in cancer is the restriction of methionine, which is an essential amino acid in one-carbon metabolism. Methionine is the most variable metabolite found in human plasma¹¹, and has a myriad of functions as a result of its location in one-carbon metabolism¹². Dietary restriction of methionine is known to extend lifespan^{13,14} and improve metabolic health^{15–17}. One-carbon metabolism, through its essential role in redox and nucleotide metabolism, is the target of frontline cancer chemotherapies such as 5-fluorouracil (5-FU), and

radiation therapy^{18–20}. Indeed, some cancer cell lines are auxotrophic for methionine²¹, and depleting or restricting methionine from the diet may have anti-cancer effects in mice^{22–24}. We therefore reasoned that methionine restriction could have broad anti-cancer properties by targeting a focused area of metabolism, and that these anti-cancer effects would interact with the response to other therapies that also affect one-carbon metabolism.

Methionine restriction alters metabolism in mouse liver and plasma after a long-term intervention¹¹, but its effect on acute time scales has not been explored in as much detail. We switched the diet of C57BL/6J male mice from chow to a control (0.86% methionine, w/w) or a methionine-restricted (0.12% methionine, w/w) diet, and obtained plasma metabolite profiles over time (Fig. 1a). We studied the metabolic dynamics using singular value decomposition (Fig. 1b, Extended Data Fig. 1a) and observed coordinated changes related to methionine and sulfur metabolism (Fig. 1b, c), which were confirmed with hierarchical clustering (Extended Data Fig. 1b). Methionine restriction reduced the levels of methionine-related metabolites within two days, and these levels were sustained throughout the intervention (Fig. 1d, Extended

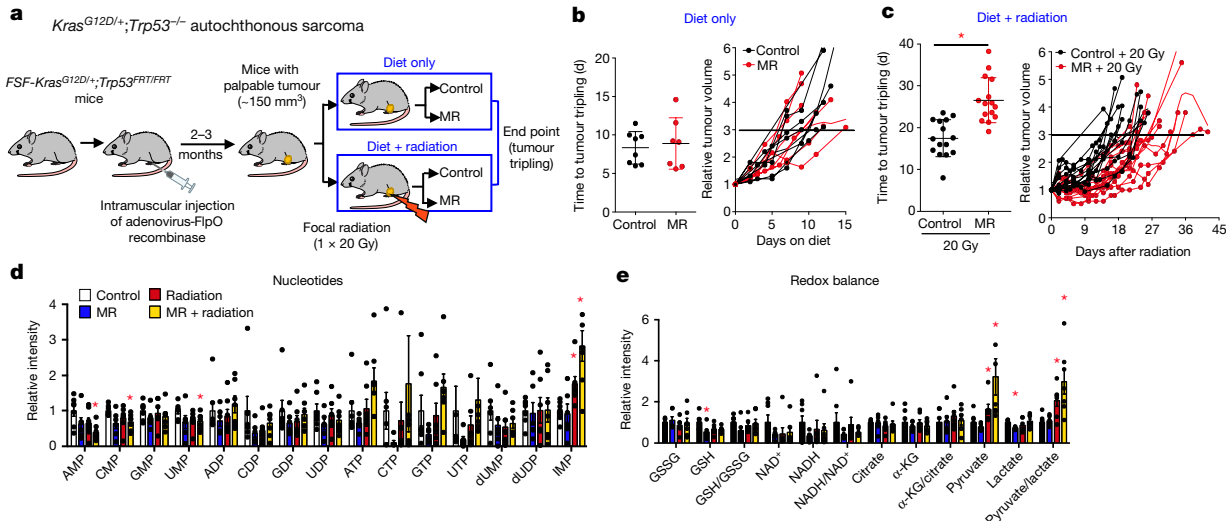


Fig. 3 | Dietary methionine restriction sensitizes mouse models of RAS-driven autochthonous sarcoma to radiation. **a**, Experimental design. **b**, Time to tumour tripling and tumour growth curve from mice on dietary treatment only. Mean ± s.d., control, $n = 8$ mice; methionine restriction, $n = 7$ mice. **c**, Time to tumour tripling and tumour growth curve from mice on the combination of dietary treatment and radiation. Mean ± s.d.,

Data Fig. 1b–f, Extended Data Table 1). Given these rapid and specific effects, we sought to evaluate methionine restriction in a series of pre-clinical settings that relate to one-carbon metabolism. We first considered two patient-derived xenograft (PDX) models of RAS-driven colorectal cancer, one of which (named CRC119) bears a KRAS(G12A) mutation and the other (named CRC240) a NRAS(Q61K) mutation (Extended Data Fig. 2a). Mice were subjected to the control or methionine-restricted diet when the tumour was palpable (for treatment settings) or two weeks before inoculation (for prevention settings) (Fig. 1e). Methionine restriction inhibited tumour growth in CRC119 ($P = 5.71 \times 10^{-12}$ at the end point, two-tailed Student's *t*-test), and showed an inhibitory effect in CRC240 ($P = 0.054$ at the end point, two-tailed Student's *t*-test) (Fig. 1f). Similar or higher amounts of food intake were observed with the methionine-restricted diet relative to the control diet (Extended Data Fig. 2b), which implies the inhibitory effect was not due to caloric restriction. To gain insights into metabolism, we profiled metabolites in tumour, plasma and liver and found that in each case methionine restriction altered methionine and sulfur-related metabolism (Extended Data Fig. 2c–e). A comparative metabolomics analysis across tissues showed that these effects most probably occur in a cell-autonomous manner (Extended Data Fig. 3, Methods), and could be confirmed with data in cell culture (Extended Data Fig. 4). Thus, the inhibition of tumour growth is at least partially (if not largely) attributable to lower circulating levels of methionine, which lead to cell-autonomous effects on tumours.

5-FU targets thymidylate synthase¹⁸ and is a frontline chemotherapy for colorectal cancer, with therapeutic strategies achieving modest (approximately 60–65%) responses^{25,26}. We therefore tested whether methionine restriction could synergize with 5-FU in the CRC119 model (Fig. 2a). We delivered a tolerable low dose of 5-FU that alone showed no effect on tumour growth (Fig. 2b). Methionine restriction synergized with 5-FU treatment, leading to a marked inhibition of tumour growth, a broad effect on metabolic pathways in tumour, plasma and liver, and, most prominently, changes to nucleotide metabolism and redox state that were related to both the mechanistic action of 5-FU and methionine restriction (Fig. 2b–d, Extended Data Fig. 5a–g). Fold changes of metabolites were highly correlated between plasma and liver (Spearman's rho = 0.38, $P = 6.7 \times 10^{-11}$) but not between tumour and liver (Spearman's rho = 0.14, $P = 0.02$) or circulation (Spearman's rho = 0.14, $P = 0.03$), which indicates that methionine restriction exerted specific effects on tumours (Extended Data Fig. 5h). Dietary

$n = 15$ mice per group. * $P < 0.05$ by two-tailed Student's *t*-test.

d, e, Relative intensity of nucleotides (**d**) and metabolites related to redox balance (**e**) in tumours. Mean ± s.e.m., $n = 7$ mice per group, except for methionine restriction ($n = 6$). * $P < 0.05$ compared to the control group by two-tailed Student's *t*-test.

restriction of methionine therefore synergizes with 5-FU, inhibiting the growth of colorectal cancer tumours and disrupting nucleotide metabolism and redox balance.

Next, we supplemented primary CRC119 cells and HCT116 colorectal cancer cells with nutrients related to methionine metabolism, in the presence of methionine restriction, 5-FU or both (Fig. 2e, Extended Data Fig. 6a, b). Nucleosides and *N*-acetylcysteine (NAC), along with related supplements, partially alleviated the inhibition of cell proliferation due to methionine restriction, both with and without 5-FU treatment, in CRC119 cells (Fig. 2f). These observations were largely replicated in HCT116 cells (Extended Data Fig. 6b). Using serine uniformly labelled with ¹³C (U-¹³C-serine), we found that methionine restriction and 5-FU led to a further reduction of [M + 1] dTTP caused by 5-FU, with an increase of [M + 1] methionine (Fig. 2g, h, Extended Data Fig. 6c). Thus, the synergistic effect between methionine restriction and 5-FU treatment is at least partially due to an increase in methionine synthesis, which competes with dTMP synthesis for the serine-derived one-carbon unit 5,10-methylene-tetrahydrofolate. These data support the conclusion that disruption to nucleotide metabolism and redox balance contributes to the inhibition of cell proliferation that is induced by methionine restriction.

To further explore the therapeutic potential of dietary restriction of methionine and related mechanisms, we considered an autochthonous mouse model of radiation resistance in soft-tissue sarcoma²⁷. Extremity sarcomas were induced in FSF-*Kras*^{G12D/+}; *Trp53*^{FRT/FRT} mice within two to three months of intramuscular delivery of adenovirus that expresses FlpO recombinase (Fig. 3a, Methods). The autochthonous and PDX models together span the spectrum of acceptable pre-clinical tumour models, and these cancer types allow for the investigation of treatments related to one-carbon metabolism (that is, chemotherapy in colorectal cancer and radiation in sarcoma). Methionine restriction alone did not alter tumour growth in this aggressive autochthonous model, and led to minimal effects on methionine metabolism (Fig. 3b, Extended Data Fig. 7a, b). Methionine restriction with a focal dose of radiation (20 Gy) reduced tumour growth and extended the tumour tripling time by 52%, from an average of 17.48 days to 26.57 days (Fig. 3c), which is comparable to effects seen with known radiosensitizing agents²⁸. These effects appeared to be tumour-cell-autonomous and not attributable to protein synthesis or methylation reactions (Extended Data Fig. 7c–e). Nevertheless, disruptions to nucleotide- and redox-related metabolism

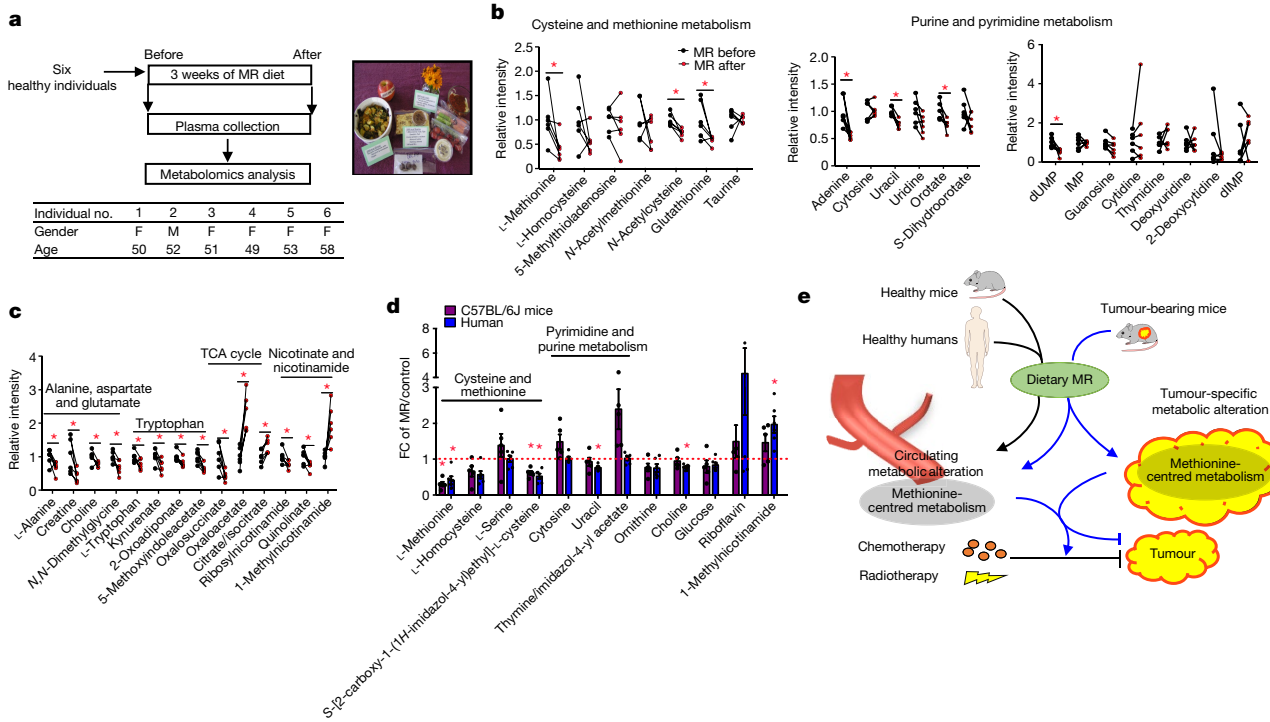


Fig. 4 | Dietary methionine restriction can be achieved in humans.

a, Experimental design, including background information on participants in the dietary study and representative daily methionine-restricted diet. **b, c**, Relative intensity of plasma metabolites related to cysteine and methionine metabolism, and purine and pyrimidine metabolism (**b**), and in the other most affected pathways (**c**). $n = 6$ individuals. * $P < 0.05$ by two-tailed Student's *t*-test.

were observed and may underlie the effects of methionine restriction in combination with radiation (Fig. 3d, e, Extended Data Fig. 7c–g).

Finally, in a proof-of-principle clinical study, we recruited six healthy middle-aged individuals and subjected them to a low methionine diet (about $2.92 \text{ mg kg}^{-1} \text{ day}^{-1}$)—equivalent to an 83% reduction in daily methionine intake—for three weeks (Fig. 4a, Methods). Methionine restriction reproducibly suppressed methionine levels and altered circulating metabolism, with cysteine and methionine metabolism among the top altered metabolic pathways (Fig. 4b, Extended Data Fig. 8a–c). Methionine restriction reduced NAC and glutathione in all subjects, and affected metabolites related to methylation, nucleotide metabolism, the tricarboxylic acid cycle and amino acid metabolism (Fig. 4b, c, Extended Data Fig. 8d). Plasma methionine-related metabolites in healthy humans were highly correlated with those in all mouse models (Spearman's rho = 0.53–0.73) (Extended Data Fig. 9a, b, Fig. 4d), which indicates that the response to methionine restriction is conserved between humans and mice. This controlled clinical study extends observations obtained from studies using methionine-free diets that are toxic^{29,30} to methionine restriction at levels that are tolerated in humans, and provide reasonable dietary possibilities—including levels of methionine that may be possible to obtain with vegan or some Mediterranean diets.

Together, we provide evidence that dietary restriction of methionine induces rapid and specific metabolic profiles in mice and humans that can be induced in a clinical setting. By disrupting the flux backbone of one-carbon metabolism with methionine restriction, vulnerabilities involving redox and nucleotide metabolism are created and can be exploited by administration of other therapies (here, radiation and antimetabolite chemotherapy) that target these aspects of cancer metabolism (Fig. 4e). Thus, a synthetic lethal interaction is defined with the diet and the otherwise-resistant treatment modality. This study may help to further establish principles of how dietary interventions may be used to influence cancer outcomes in broader contexts.

two-tailed Student's *t*-test. **d**, Methionine-restriction-induced fold changes of plasma metabolites in cysteine and methionine metabolism, and pyrimidine and purine metabolism in C57BL/6J mice ($n = 5$) and humans ($n = 6$). Mean \pm s.e.m. * $P < 0.05$ by two-tailed Student's *t*-test. **e**, Model of the influence of dietary methionine restriction on tumour-cell metabolism.

Online content

Any methods, additional references, Nature Research reporting summaries, source data, extended data, supplementary information, acknowledgements, peer review information; details of author contributions and competing interests; and statements of data and code availability are available at <https://doi.org/10.1038/s41586-019-1437-3>.

Received: 27 July 2018; Accepted: 26 June 2019;
Published online 31 July 2019.

- DeBerardinis, R. J. & Chandel, N. S. Fundamentals of cancer metabolism. *Sci. Adv.* **2**, e1600200 (2016).
- Goncalves, M. D., Hopkins, B. D. & Cantley, L. C. Dietary fat and sugar in promoting cancer development and progression. *Annual Rev. Cancer Biol.* **3**, 255–273 (2019).
- Cantor, J. R. et al. Physiologic medium rewires cellular metabolism and reveals uric acid as an endogenous inhibitor of UMP synthase. *Cell* **169**, 258–272 (2017).
- Tardito, S. et al. Glutamine synthetase activity fuels nucleotide biosynthesis and supports growth of glutamine-restricted glioblastoma. *Nat. Cell Biol.* **17**, 1556–1568 (2015).
- Liu, X., Romero, I. L., Litchfield, L. M., Lengyel, E. & Locasale, J. W. Metformin targets central carbon metabolism and reveals mitochondrial requirements in human cancers. *Cell Metab.* **24**, 728–739 (2016).
- Maddock, O. D. et al. Serine starvation induces stress and p53-dependent metabolic remodelling in cancer cells. *Nature* **493**, 542–546 (2013).
- Maddock, O. D. K. et al. Modulating the therapeutic response of tumours to dietary serine and glycine starvation. *Nature* **544**, 372–376 (2017).
- Gravel, S. P. et al. Serine deprivation enhances antineoplastic activity of biguanides. *Cancer Res.* **74**, 7521–7533 (2014).
- Kanarek, N. et al. Histidine catabolism is a major determinant of methotrexate sensitivity. *Nature* **559**, 632–636 (2018).
- Knott, S. R. V. et al. Asparagine bioavailability governs metastasis in a model of breast cancer. *Nature* **554**, 378–381 (2018).
- Mentch, S. J. et al. Histone methylation dynamics and gene regulation occur through the sensing of one-carbon metabolism. *Cell Metab.* **22**, 861–873 (2015).
- Gao, X., Reid, M. A., Kong, M. & Locasale, J. W. Metabolic interactions with cancer epigenetics. *Mol. Aspects Med.* **54**, 50–57 (2017).
- Orentreich, N., Matias, J. R., DeFelice, A. & Zimmerman, J. A. Low methionine ingestion by rats extends life span. *J. Nutr.* **123**, 269–274 (1993).

14. Lee, B. C. et al. Methionine restriction extends lifespan of *Drosophila melanogaster* under conditions of low amino-acid status. *Nat. Commun.* **5**, 3592 (2014).
15. Malloy, V. L. et al. Methionine restriction prevents the progression of hepatic steatosis in leptin-deficient obese mice. *Metabolism* **62**, 1651–1661 (2013).
16. Ables, G. P., Perrone, C. E., Orentreich, D. & Orentreich, N. Methionine-restricted C57BL/6J mice are resistant to diet-induced obesity and insulin resistance but have low bone density. *PLoS ONE* **7**, e51357 (2012).
17. Malloy, V. L. et al. Methionine restriction decreases visceral fat mass and preserves insulin action in aging male Fischer 344 rats independent of energy restriction. *Aging Cell* **5**, 305–314 (2006).
18. Ser, Z. et al. Targeting one carbon metabolism with an antimetabolite disrupts pyrimidine homeostasis and induces nucleotide overflow. *Cell Reports* **15**, 2367–2376 (2016).
19. Miousse, I. R. et al. One-carbon metabolism and ionizing radiation: a multifaceted interaction. *Biomol. Concepts* **8**, 83–92 (2017).
20. Locasale, J. W. Serine, glycine and one-carbon units: cancer metabolism in full circle. *Nat. Rev. Cancer* **13**, 572–583 (2013).
21. Hoffman, R. M. & Erbe, R. W. High *in vivo* rates of methionine biosynthesis in transformed human and malignant rat cells auxotrophic for methionine. *Proc. Natl Acad. Sci. USA* **73**, 1523–1527 (1976).
22. Komninou, D., Leutzinger, Y., Reddy, B. S. & Richie, J. P. Jr. Methionine restriction inhibits colon carcinogenesis. *Nutr. Cancer* **54**, 202–208 (2006).
23. Hens, J. R. et al. Methionine-restricted diet inhibits growth of MCF10AT1-derived mammary tumors by increasing cell cycle inhibitors in athymic nude mice. *BMC Cancer* **16**, 349 (2016).
24. Guo, H. et al. Therapeutic tumor-specific cell cycle block induced by methionine starvation *in vivo*. *Cancer Res.* **53**, 5676–5679 (1993).
25. Saltz, L. B. et al. Bevacizumab in combination with oxaliplatin-based chemotherapy as first-line therapy in metastatic colorectal cancer: a randomized phase III study. *J. Clin. Oncol.* **26**, 2013–2019 (2008).
26. Douillard, J. Y. et al. Randomized, phase III trial of panitumumab with infusional fluorouracil, leucovorin, and oxaliplatin (FOLFOX4) versus FOLFOX4 alone as first-line treatment in patients with previously untreated metastatic colorectal cancer: the PRIME study. *J. Clin. Oncol.* **28**, 4697–4705 (2010).
27. Kirsch, D. G. et al. A spatially and temporally restricted mouse model of soft tissue sarcoma. *Nat. Med.* **13**, 992–997 (2007).
28. Moding, E. J. et al. Tumor cells, but not endothelial cells, mediate eradication of primary sarcomas by stereotactic body radiation therapy. *Sci. Transl. Med.* **7**, 278ra34 (2015).
29. Durando, X. et al. Optimal methionine-free diet duration for nitrourea treatment: a phase I clinical trial. *Nutr. Cancer* **60**, 23–30 (2008).
30. Durando, X. et al. Dietary methionine restriction with FOLFOX regimen as first line therapy of metastatic colorectal cancer: a feasibility study. *Oncology* **78**, 205–209 (2010).

Publisher's note: Springer Nature remains neutral with regard to jurisdictional claims in published maps and institutional affiliations.

© The Author(s), under exclusive licence to Springer Nature Limited 2019

METHODS

No statistical methods were used to predetermine sample size.

Animals, diets and tissue collection. All animal procedures and studies were approved by the Institutional Animal Care and Use Committee (IACUC) at Duke University. All experiments were performed in accordance with relevant guidelines and regulations. All mice were housed at $20 \pm 2^\circ\text{C}$ with $50 \pm 10\%$ relative humidity and a standard 12-h dark–12-h light cycle. The special diets with defined methionine levels that have previously been used^{11,16} were purchased from Research Diets; the control diet contained 0.86% methionine (w/w, catalogue no. A11051302) and methionine-restricted diet contained 0.12% methionine (w/w, catalogue no. A11051301). Three mouse models were used, and are described in ‘PDX models of colorectal cancer’ and ‘Autochthonous soft-tissue sarcomas’. For all animal studies, mice were randomized to the control or methionine-restricted diet, and investigators were not blinded to allocation during experiments or outcome assessment. **Methionine-restriction time-course study in healthy mice.** Twelve-week-old male C57BL/6J mice (Jackson Laboratories) were subjected to either the control or the methionine-restricted diet ad libitum for three weeks. Mouse blood was sampled through tail bleeding in the morning (10:00–12:00) at days 1, 2, 4, 7, 10, 14, 17 and 21 after the dietary treatments. By day 21, all mice were euthanized for tissue collection.

PDX models of colorectal cancer. PDX models of colorectal cancer with liver metastasis were developed as previously described^{31,32}, under an IRB-approved protocol (Pro00002435). In brief, CRC119 and CRC240 tumours were resected, washed and minced, and then passaged through JAX NOD.CB17-PrkdcSCID-J mice 2–5 times. For the dietary studies, CRC119 and CRC240 PDX tumours were minced in PBS at 150 mg/ml and 200 μl of tumour suspension was subcutaneously injected into the flanks of NOD.Cg-Prkdc^{cid} Il2rg^{tm1Wjl}/SzJ mice from the Jackson Laboratory. Mice (four female and three or four male) were subjected to the control or methionine-restricted diet, either two weeks before the tumour injection or from when the tumour was palpable until the end point (a tumour volume of about 1,500 mm^3). Tumour size was monitored two to three times per week until the end point. For the combination therapy with the standard chemotherapy drug 5-FU, mice were subjected to the control or the methionine-restricted diet from two weeks before the tumour injection until the end point. When tumours were palpable, mice (four female and four male) were randomized to treatment of 5-FU (NDC 63323-117-10, 12.5 mg/kg three times per week) or vehicle (saline) through intraperitoneal injection. To minimize toxicity, we delivered an established low dose of 5-FU³³. Tumour size was monitored two to three times per week until the end point.

Autochthonous soft-tissue sarcomas. Primary soft-tissue sarcomas were generated as previously described^{27,34}. In brief, *Trp53*^{FRT} mice were crossed with mice that carry an Flp-activated allele of oncogenic *Kras* (*FSF-Kras*^{G12D}) to generate *FSF-Kras*^{G12D/+}; *Trp53*^{FRT/FRT} compound conditional-mutant mice (KP mice). *Trp53*^{FRT} mice and *FSF-Kras*^{G12D} mice were maintained on mixed C57BL/6J × 129SvJ backgrounds. Soft-tissue sarcomas were induced by intramuscular injection of an adenovirus that expresses FlpO into KP mice. Twenty-five microlitres of Ad5CMVFlpO (6×10^{10} plaque-forming units per millilitre) was incubated with 600 μl minimum essential medium (Sigma-Aldrich) and 3 μl 2 M CaCl₂ (Sigma-Aldrich) for 15 min to form calcium phosphate precipitates. Fifty microlitres of precipitated virus was injected intramuscularly per mouse to generate sarcomas. Soft-tissue sarcomas developed at the site of injection in the lower extremity as early as two months after injection. *FSF-Kras*^{G12D} mice were provided by T. Jacks at MIT, and *Trp53*^{FRT} mice had previously been generated at Duke University^{27,34}.

KP mice (of mixed sex) were subjected to a control or methionine-restricted diet when tumours were palpable (about 150 mm^3), until the end point when the tumour tripled in size. Tumour size was monitored two or three times per week. For combination therapy with radiation, KP mice with palpable tumours were subjected to a single dose of 20 Gy focal radiation, which is moderately effective in this model³⁵, using the X-RAD 225Cx small-animal image-guided irradiator (Precision X-Ray). The irradiation field was centred on the target via fluoroscopy with 40-kilovolt peak (kVp), 2.5-mA X-rays using a 2-mm aluminium filter. Sarcomas were irradiated with parallel-opposed anterior and posterior fields with an average dose rate of 300 cGy/min prescribed to midplane with 225-kVp, 13-mA X-rays using a 0.3-mm copper filter and a collimator with a 40 × 40-mm² radiation field at the treatment isocentre. The dose rate was monitored in an ion chamber by members of the Radiation Safety Division at Duke University. After radiation, mice were immediately subjected to the control or the methionine-restricted diet until the end point at which the tumour tripled in size. Tissues (tumour, liver and plasma) were collected at the time of tumour tripling. For metabolomics analysis, another cohort of mice on the combination therapy with radiation was euthanized at ten days after the radiation and dietary treatment (the average time point at which the tumour size tripled in the KP mice on the control or the methionine-restricted diet alone).

Tissue collection. For tissue collection from all the above mouse studies, mice were fasted in the morning for four hours (9:00–13:00). Tumour, plasma and liver were collected and then immediately snap-frozen, and stored at -80°C until processed. **Colorectal cancer cell lines.** Early-passage primary CRC119 and CRC240 colorectal cancer cell lines were developed from the PDXs. PDXs were collected and homogenized, and the homogenates were grown in RPMI 1640 medium with addition of 10% fetal calf serum, 100,000 U/l penicillin and 100 mg/l streptomycin at 5% CO₂. A single-cell clone was isolated using an O ring. The HCT116 cell line was a gift from the laboratory of L. Cantley, and was maintained in RPMI 1640 supplemented with 10% fetal bovine serum and 100,000 U/l penicillin and 100 mg/l streptomycin. Cells were grown at 37°C with 5% CO₂. Cell lines were authenticated and tested for mycoplasma at the Duke University DNA Analysis Facility by analysing DNA samples from each cell lines for polymorphic short tandem repeat markers using the GenePrint 10 kit from Promega. All cell lines were negative for mycoplasma contamination.

Cell viability assay. Cell viability was determined by MTT (Invitrogen) assays. In brief, cells cultured in 96-well plates were incubated in RPMI medium containing MTT (final concentration 0.5 mg/ml) in a cell incubator for 2–4 h. The medium was then removed and replaced with 100 μl DMSO, followed by additional 10 min of incubation at 37°C . The absorbance at 540 nm was read using a plate reader. For the metabolite rescue studies, 10 μM methionine (one tenth of the amount in the RPMI medium) was used to approximately model dietary methionine restriction. We evaluated the effects of supplementation of a suite of nutrients related to methionine metabolism, and the observed differences in metabolite profiles of the mouse models of colorectal cancer—including the one-carbon donors choline and formate; the sulfur donor homocysteine, with or without cofactor vitamin B12; nucleosides; and the antioxidant NAC—on methionine restriction alone or in combination with 5-FU treatment caused defects in cell proliferation. The following final conditions of metabolites were used: homocysteine (400 μM), vitamin B12 (20 μM), nucleosides (Millipore, 1×), choline (1 mM), formate (0.5 mM), NAC (1 mM) and 5-FU (2.5 μM).

Human dietary study. The controlled feeding study was conducted at Penn State University Clinical Research Center and approved by the IRB of the Penn State College of Medicine, in accordance with the Helsinki Declaration of 1975 as revised in 1983 (IRB no. 32378). We have complied with all relevant ethical regulations. Healthy adults of mixed gender were recruited by fliers and word of mouth and—as assessed for initial eligibility by telephone interview—were free of disease and not currently taking specific medications (including anti-inflammatory drugs, corticosteroids, statins, thyroid drugs and oral contraceptives). Final eligibility was assessed by standard clinical chemistry and haematology analyses. Written consent was obtained from eligible subjects and baseline resting metabolic rate was assessed by indirect calorimetry (Parvo Medics), physical activity by questionnaire and dietary intake by 3 unannounced 24-h diet recalls conducted by telephone in the week before returning to the clinic. All of the subjects—6 healthy adults (5 women and 1 man) with a mean ± s.d. age of 52.2 ± 3.19 years (range of 49–58 years) and body mass index of $27.6 \pm 4.32 \text{ kg/m}^2$ —were placed on an methionine-restricted diet for the final 3 weeks, which provided 50–53% of energy from carbohydrate, 35–38% from fat and 12–13% from protein; total calories were adjusted individually on the basis of the baseline of resting metabolic rate and physical activity (calculated by the Harris Benedict Equation). Of the total protein, 75% was provided by a methionine-free medicinal beverage (Hominex-2, Abbott Nutrition) and the remaining 25% was from low-methionine foods such as fruits, vegetables and refined grains. The total methionine intake was about 2.92 mg kg⁻¹ day⁻¹, which represented an 83% reduction in methionine intake compared to pre-test values from diet recalls (about 17.2 mg kg⁻¹ day⁻¹ at baseline level). The five-day-cycle menu was created and evaluated for nutrient content using the Nutrition Data System for Research. Blood was sampled by a registered nurse into EDTA tubes in the morning after overnight fasting, at the beginning and end of the diet period. Plasma was obtained after centrifugation at 5,000 r.p.m. for 10 min at 4°C. All six subjects agreed to have their samples and data used for future research. Biosamples were anonymized by re-coding. There was no registration or pre-registration of this study.

Metabolite profiling and isotope tracing. PDX primary cell lines were seeded in 6-well plates at a density of 2.0×10^5 cells per well. For overall polar metabolite profile, after overnight incubation cells were washed once with PBS and cultured for an additional 24 h with 2 ml of conditional RPMI medium containing 0 μM or 100 μM methionine plus 10% FBS. Cellular metabolites were extracted after incubation. For U-¹³C-serine isotope tracing, both primary CRC119 cells and HCT116 cells were seeded in 6-well plates at a density of 2.0×10^5 cells per well. Cells were washed once with PBS after overnight incubation, and cultured for an additional 24 h with 2 ml of conditional RPMI medium containing 0 μM or 100 μM methionine with or without addition of 5-FU (3.4 or 10 μM) plus 10% FBS. Then, medium was replaced with fresh conditional RPMI medium (0 μM or 100 μM methionine) with or without addition of 5-FU (3.4 or 10 μM) containing tracer U-¹³C-serine plus

10% dialysed FBS. Cells were traced for 6 h, and tracing was followed by cellular metabolite extraction.

Metabolite extraction. Polar metabolite extraction has previously been described³⁶. In brief, tissue samples (liver and tumour) were pulverized in liquid nitrogen and then 3–10 mg of each was weighed out for metabolite extraction using ice-cold extraction solvent (80% methanol/water, 500 µl). Tissue was then homogenized with a homogenizer to an even suspension, and incubated on ice for an additional 10 min. The extract was centrifuged at 20,000g for 10 min at 4°C. The supernatant was transferred to a new Eppendorf tube and dried in vacuum concentrator. For serum or medium, 20 µl of sample was added to 80 µl ice-cold water in an Eppendorf tube on ice, followed by the addition of 400 µl ice-cold methanol. Samples were vortexed at the highest speed for 1 min before centrifugation at 20,000g for 10 min at 4°C. For cells cultured in 6-well plates, cells were placed on top of dry ice right after medium removal. One millilitre ice-cold extraction solvent (80% methanol/water) was added to each well and the extraction plate was quenched at –80°C for 10 min. Cells were then scraped off the plate into an Eppendorf tube. Samples were vortexed and centrifuged at 20,000g for 10 min at 4°C. The supernatant was transferred to a new Eppendorf tube and dried in vacuum concentrator. The dry pellets were stored at –80°C for liquid chromatography with high-resolution mass spectrometry analysis. Samples were reconstituted into 30–60 µl sample solvent (water:methanol:acetonitrile, 2:1:1, v/v/v) and were centrifuged at 20,000g at 4°C for 3 min. The supernatant was transferred to liquid chromatography vials. The injection volume was 3 µl for hydrophilic interaction liquid chromatography (HILIC), which is equivalent to a metabolite extract of 160 µg tissue injected on the column.

High-performance liquid chromatography. An Ultimate 3000 UHPLC (Dionex) was coupled to Q Exactive-Mass spectrometer (QE-MS, Thermo Scientific) for metabolite separation and detection. For additional polar metabolite analysis, a HILIC method was used, with an Xbridge amide column (100 × 2.1 mm internal diameter, 3.5 µm; Waters), for compound separation at room temperature. The mobile phase and gradient information has previously been described³⁷.

Mass spectrometry and data analysis. The QE-MS was equipped with a HESI probe, and the relevant parameters were: heater temperature, 120°C; sheath gas, 30; auxiliary gas, 10; sweep gas, 3; spray voltage, 3.6 kV for positive mode and 2.5 kV for negative mode. Capillary temperature was set at 320°C, and the S-lens was 55. A full scan range was set at 60 to 900 (*m/z*) when coupled with the HILIC method, or 300 to 1,000 (*m/z*) when low-abundance metabolites needed to be measured. The resolution was set at 70,000 (at *m/z* 200). The maximum injection time was 200 ms. Automated gain control was targeted at 3 Å ~ 10⁶ ions. Liquid chromatography-mass spectrometry peak extraction and integration were analysed with commercially available software Sieve 2.0 (Thermo Scientific). The integrated peak intensity was used for further data analysis. For tracing studies using U-¹³C-serine, ¹³C natural abundance was corrected as previously described³⁸.

Statistical analysis and bioinformatics. Pathway analysis of metabolites was carried out with software MetaboAnalyst (<http://www.metaboanalyst.ca/MetaboAnalyst/>) using the Kyoto Encyclopedia of Genes and Genomes (KEGG) pathway database (<http://www.genome.jp/kegg/>). All data are represented as mean ± s.d. or mean ± s.e.m. as indicated. *P* values were calculated by a two-tailed Student's *t* test unless otherwise noted.

Analysis of the time-course metabolomics data. We first constructed a combinational matrix that contained the raw ion intensities of plasma metabolites from C57BL/6J mice (both the control and the methionine-restriction groups). For each group, there were 9 time points and 5 replicates for each time point, which resulted in a 311 × 90 matrix. This matrix was then log-transformed and iteratively row-normalized and column-normalized until the mean values of all rows and columns converged to zero. Singular value decomposition³⁹ was applied on the processed matrix to identify dominating dynamic modes:

$$A = U\Sigma V^T = \sum_{i=1}^r \sigma_i \mathbf{u}_i \mathbf{v}_i^T$$

in which A is the processed metabolomics matrix, σ_i is the *i*th singular value (ranked from maximal to minimal), and $\sigma_i \mathbf{v}_i^T$ is termed the *i*th mode. Elements of \mathbf{u}_i (that is, the *i*th column vector of U) are coefficients for the *i*th mode. Modes 2 and 3 were defined as responding modes, owing to the significant difference between control and methionine-restriction values in both modes. For the *i*th metabolite, the total contribution of modes 2 and 3 to its dynamics was evaluated by: $C_{23,i} = \mathbf{u}_{i2}^2 + \mathbf{u}_{i3}^2$. Mode 1 reflected an overall metabolic change due to switching diets at time zero. Modes 2 and 3 predominantly contained metabolites related to methionine and sulfur metabolism. Time-course metabolomics data of 50 metabolites with highest contribution of modes 2 and 3 were then clustered using the clustergram() function in MATLAB R2018b. All methods used were implemented in MATLAB code. Hierarchical clustering confirmed that a set of

methionine-related metabolites was most rapidly suppressed, with other compensatory pathways changing at later times.

Cross-tissue comparison of metabolite fold changes in PDX and sarcoma models. Spearman's rank correlation coefficients were computed on metabolites measured in plasma, tumour and liver. The distance between fold changes in tissues A and B (for example, liver and tumour) was computed by measuring the Euclidean distance between the two vectors of the fold changes that contained all metabolites measured in both A and B. Multidimensional scaling was then applied to visualize the tissues in two dimensions; a stress function, which measures the difference between the dimension-reduced values and the values in the original dataset, was minimized:

$$\min \text{Stress}(\mathbf{x}_1, \dots, \mathbf{x}_N) = \left(\frac{\sum_{ij} (d_{ij} - \|\mathbf{x}_i - \mathbf{x}_j\|)^2}{\sum_{ij} d_{ij}^2} \right)^{1/2}$$

$$\mathbf{x}_1, \dots, \mathbf{x}_N \in \mathbb{R}^2$$

in which N is the total number of metabolites used in the original dataset, d_{ij} is the Euclidean distance between the *i*th and *j*th data points in the original dataset, and \mathbf{x}_i is the *i*th point in the dimension-reduced dataset. All methods used here were implemented in MATLAB.

Methionine-related and methionine-unrelated metabolites. To determine whether the effect of methionine restriction on tumour growth is systemic, cell autonomous or both, we conducted an integrated analysis of global changes in the metabolic network across tumour, plasma and liver within each model from the prevention study in PDX models of colorectal cancer in Fig. 1f. Methionine-related and -unrelated metabolites were defined according to their distance to methionine in the genome-scale metabolic human model Recon 2 (ref. ⁴⁰). Metabolites were defined as methionine-related if the distance to methionine was less than or equal to four, or methionine-unrelated when the distance to methionine was larger than four. Metabolites were mapped by their KEGG identity between the metabolomics dataset and Recon 2.

Quantification of methionine concentrations. To quantify methionine concentrations in plasma, liver and tumour across the mouse models and in healthy humans, two additional datasets of metabolomics profiles in human plasma with their corresponding absolute methionine concentrations (quantified using ¹³C-labelled standards) were used. The raw intensities across all samples were log-transformed and normalized. Linear regression was then performed on the normalized datasets to predict absolute methionine concentrations. Four normalization algorithms including cyclic loess, quantile, median and *z*-score were tested. Among the normalization algorithms, cyclic loess had the highest *R*² statistics in the corresponding linear regression model (*R*² = 0.74 for cyclic loess compared to 0.66 for quantile, 0.68 for median and 0.70 for *z*-score). Thus, the cyclic-loess-normalized dataset was used for the final model training, which generated the following equation describing the model: $\log(\text{methionine concentration}) = 1.001676 \log(I_{\text{methionine}}) - 14.446017$. In this equation, methionine concentration refers to the absolute methionine concentration, and $I_{\text{methionine}}$ is the cyclic-loess-normalized value of methionine intensity.

Reporting summary. Further information on research design is available in the Nature Research Reporting Summary linked to this paper.

Data availability

The metabolomics data reported in this study have been deposited in Mendeley Data (<https://doi.org/10.17632/zs269d9fvb.1>).

Code availability

All computer code is available at: https://github.com/LucasaleLab/Dietary_methionine_restriction.

31. Kim, M. K. et al. Characterization of an oxaliplatin sensitivity predictor in a preclinical murine model of colorectal cancer. *Mol. Cancer Ther.* **11**, 1500–1509 (2012).
32. Uronis, J. M. et al. Histological and molecular evaluation of patient-derived colorectal cancer explants. *PLoS ONE* **7**, e38422 (2012).
33. Udofo, O. et al. Pharmacokinetic, biodistribution and therapeutic efficacy of 5-fluorouracil-loaded pH-sensitive PEGylated liposomal nanoparticles in HCT-116 tumor bearing mouse. *J. Natl. Sci.* **2**, e171 (2016).
34. Lee, C. L. et al. Generation of primary tumors with Flp recombinase in *FRT*-flanked *p53* mice. *Dis. Model. Mech.* **5**, 397–402 (2012).
35. Moding, E. J. et al. *Atm* deletion with dual recombinase technology preferentially radiosensitizes tumor endothelium. *J. Clin. Invest.* **124**, 3325–3338 (2014).
36. Liu, X. et al. High-resolution metabolomics with acyl-CoA profiling reveals widespread remodeling in response to diet. *Mol. Cell. Proteomics* **14**, 1489–1500 (2015).

37. Liu, X., Ser, Z. & Locasale, J. W. Development and quantitative evaluation of a high-resolution metabolomics technology. *Anal. Chem.* **86**, 2175–2184 (2014).
38. Yuan, J., Bennett, B. D. & Rabinowitz, J. D. Kinetic flux profiling for quantitation of cellular metabolic fluxes. *Nat. Protocols* **3**, 1328–1340 (2008).
39. Holter, N. S. et al. Fundamental patterns underlying gene expression profiles: simplicity from complexity. *Proc. Natl Acad. Sci. USA* **97**, 8409–8414 (2000).
40. Thiele, I. et al. A community-driven global reconstruction of human metabolism. *Nat. Biotechnol.* **31**, 419–425 (2013).

Acknowledgements We gratefully acknowledge support from the National Institutes of Health (NIH) R01CA193256, R21CA201963 and P30CA014236 (J.W.L.), R35CA197616 (D.G.K.), T32CA93240 (D.E.C.) and the Canadian Institutes of Health Research (CIHR) 146818 (X.G.). We thank M. L. Kiel and T. Hartman for assistance in designing the diets, and S. Heim for help with food preparation in the human study. The human study was partially supported by the Clinical Research Center at Penn State University (NIH M01RR10732). We gratefully acknowledge members of the Locasale laboratory for discussions and apologize to those whose work we could not cite owing to space constraints.

Author contributions X.G. and J.W.L. designed the study, wrote and edited the paper. D.E.C. and D.G.K. designed the sarcoma experiments and edited

the paper. M.L. and D.S.H. designed and implemented the colorectal PDX models and edited the paper. X.G., M.L., D.E.C., G.A. and M.A.R. performed animal experiments. X.G., S.M.S. and M.A.R. performed all cell culture experiments. J.P.R. Jr, A. Ciccarella, A. Calcagnotto and S.N.N. conducted the human study. Z.D. conducted computational analyses with initial help from P.G.M. J.L. and S.J.M. assisted in mass spectrometry metabolomics experiments.

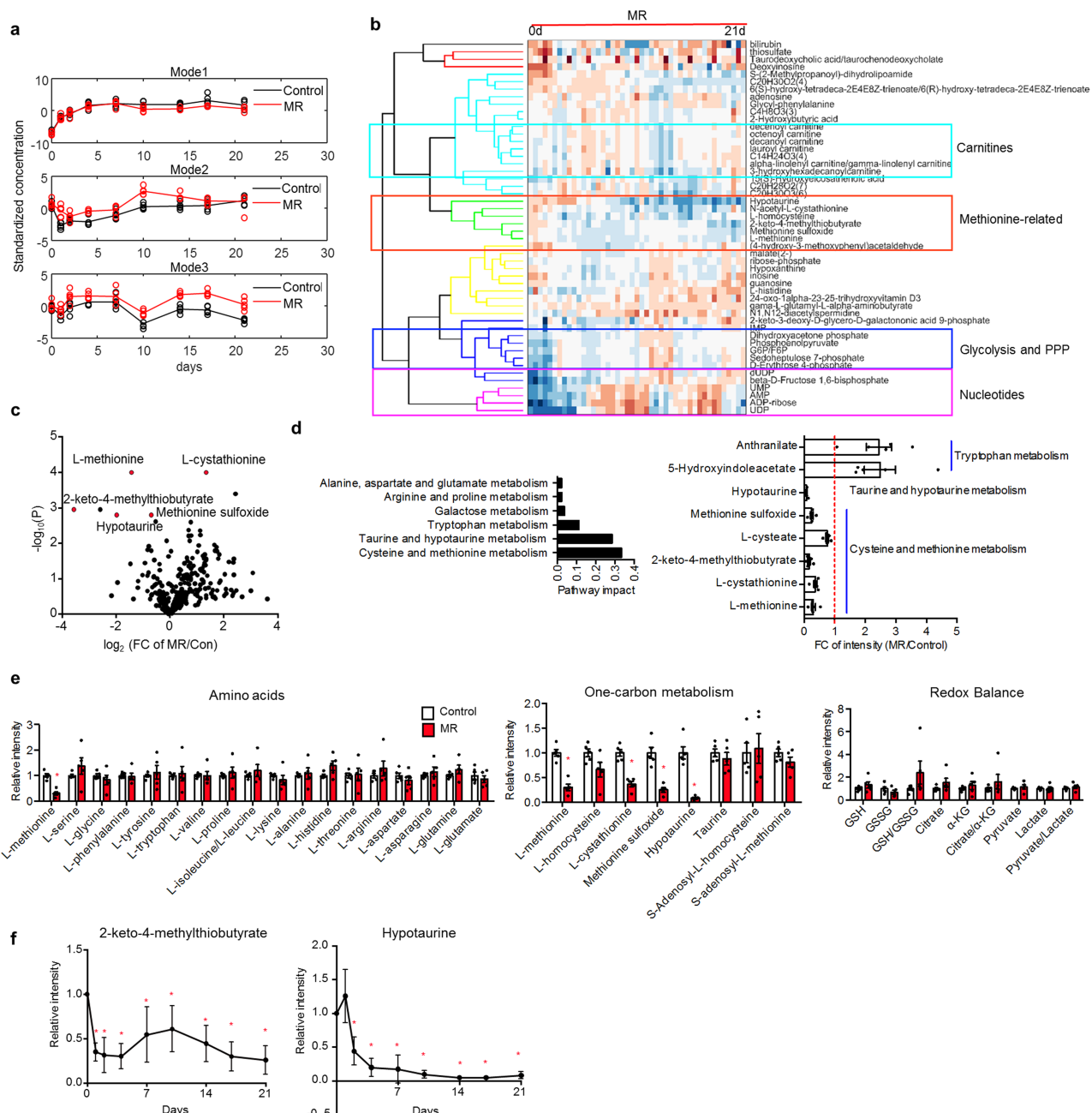
Competing interests J.W.L. and X.G. have patents related to targeting amino acid metabolism in cancer therapy. D.G.K. is a co-founder and has equity in XRAD Therapeutics, a company developing radiosensitizing agents. He also has patents related to radiosensitizing agents.

Additional information

Supplementary information is available for this paper at <https://doi.org/10.1038/s41586-019-1437-3>.

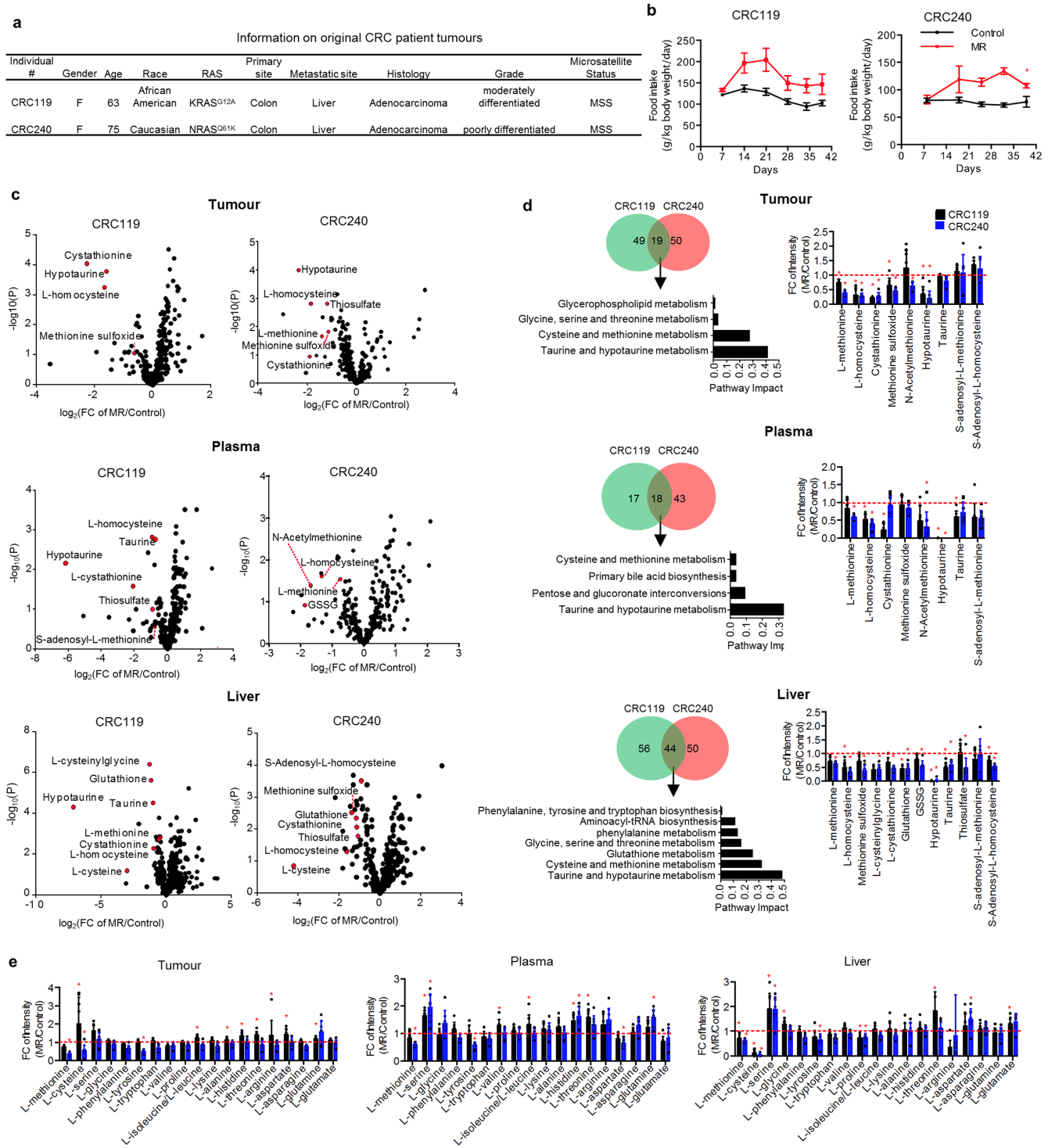
Correspondence and requests for materials should be addressed to J.W.L. **Peer review information** *Nature* thanks Danica Chen, Naama Kanarek and Alexei Vazquez for their contribution to the peer review of this work.

Reprints and permissions information is available at <http://www.nature.com/reprints>.



Extended Data Fig. 1 | Dietary restriction of methionine rapidly and specifically alters methionine and sulfur metabolism but maintains overall metabolism in healthy C57BL/6J mice. **a**, Dynamic patterns of the top three modes. Standardized concentration (the values are normalized to have mean = 0, s.d. = 1) in mode 1, mode 2 and mode 3. **b**, Heat map of metabolites in mode 2 and mode 3. PPP, pentose phosphate pathway. **c**, Volcano plot of metabolites in plasma collected at the end point. *P* values were determined by two-tailed Student's *t*-test. **d**, Left, pathway analysis of significantly changed (**P* < 0.05, two-tailed

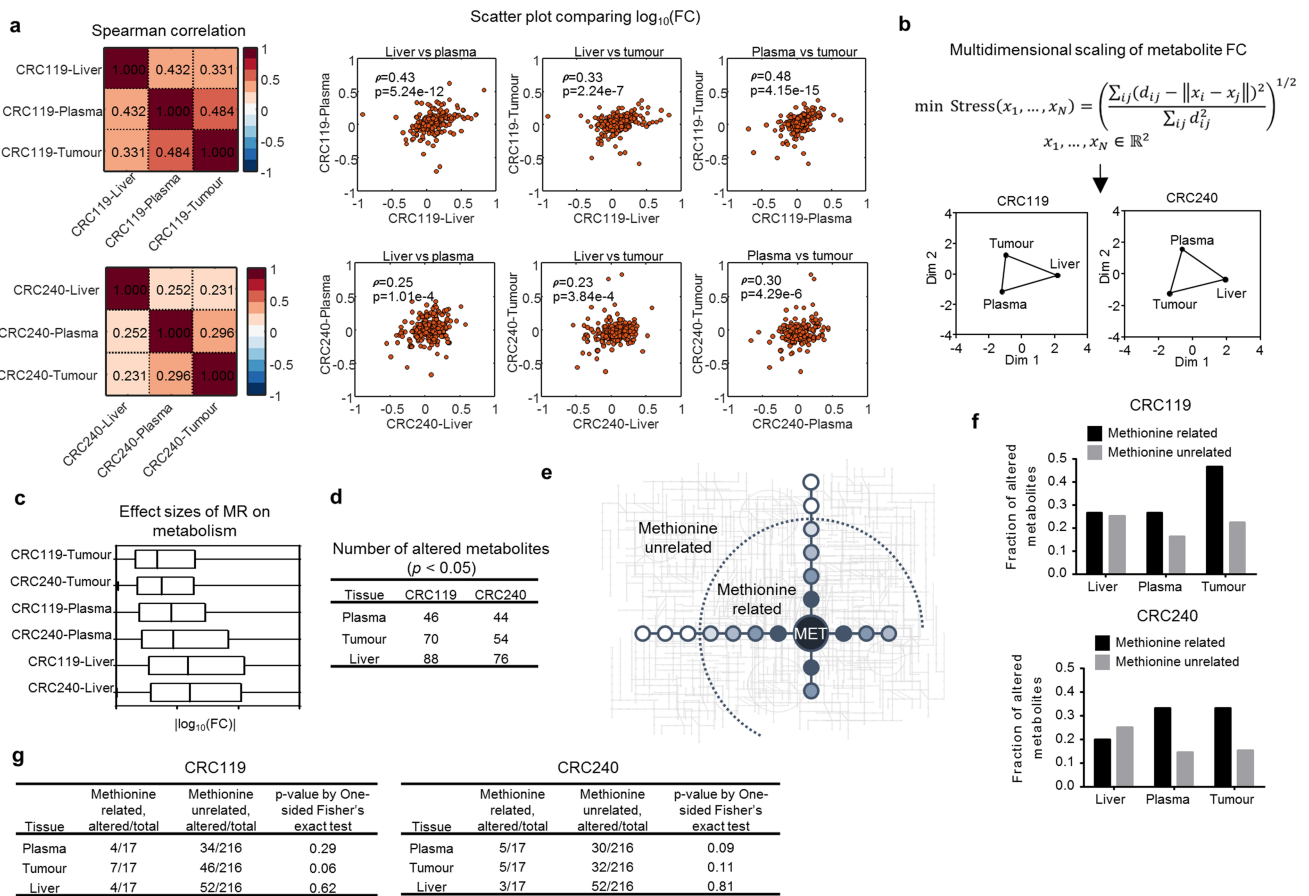
Student's *t*-test) plasma metabolites by 21-day methionine-restricted diet. Right, fold change of altered metabolites in the top three most-affected pathways. Mean \pm s.e.m., $n = 5$ mice per group. * $P < 0.05$, two-tailed Student's *t*-test. **e**, Relative intensity of plasma amino acids and metabolites in one-carbon metabolism and redox balance at the end of the study. Mean \pm s.e.m., $n = 5$ mice per group. * $P < 0.05$, two-tailed Student's *t*-test. **f**, Relative intensity of the methionine-metabolism-related metabolites 2-keto-4-methylthiobutyrate and hypotaurine. Mean \pm s.d., $n = 5$ mice per group. * $P < 0.05$, two-tailed Student's *t*-test.



Extended Data Fig. 2 | Dietary restriction of methionine alters methionine metabolism in PDX models of colorectal cancer.

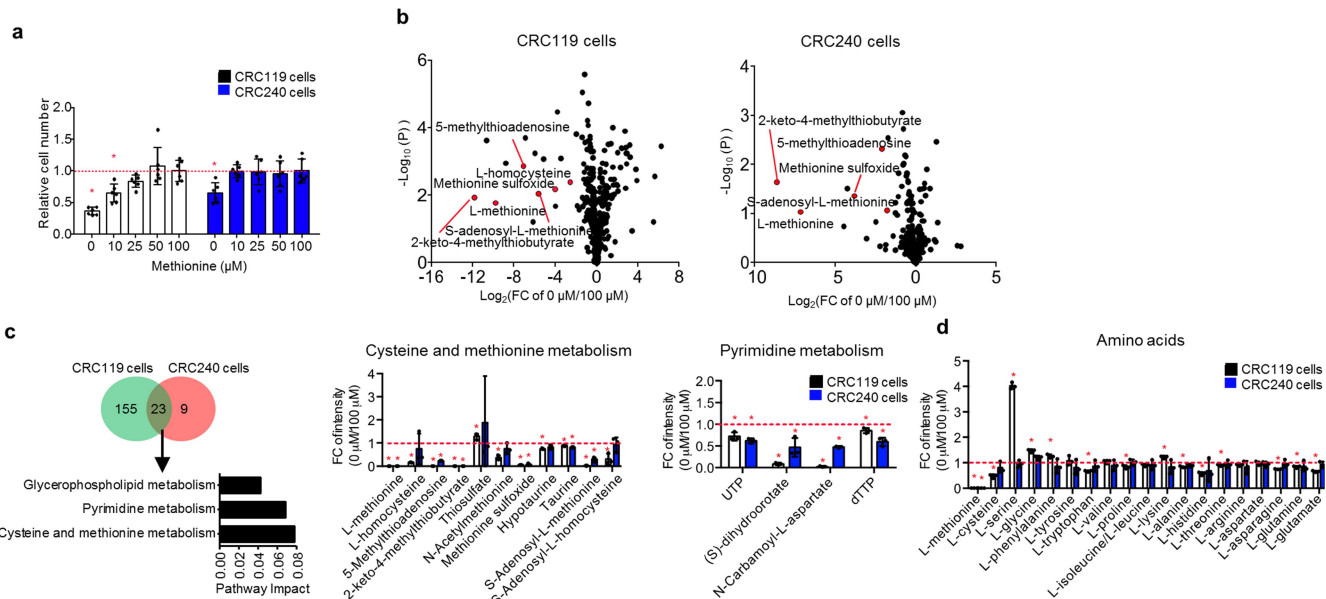
a, Information on original tumours from patients with colorectal cancer.
 b–e, Data from the prevention study shown in Fig. 1f. $n = 8$ mice per group (4 female and 4 male). b, Food intake. Mean \pm s.e.m. * $P < 0.05$, two-tailed Student's t -test. c, Volcano plots of metabolites in tumour, plasma and liver. P values were determined by two-tailed Student's t -test.
 d, Left, Venn diagrams of significantly changed (* $P < 0.05$, two-tailed Student's t -test) metabolites in tumour, plasma and liver by methionine

restriction and pathway analysis (false discovery rate < 0.5) of the commonly changed metabolites. Right, fold changes of intensity of tumour metabolites in cysteine and methionine metabolism, and taurine and hypotaurine metabolism, induced by methionine restriction. Mean \pm s.d. * $P < 0.05$, two-tailed Student's t -test. $n = 8$ mice per group (4 female and 4 male). e, Relative fold change of intensity of amino acids. Mean \pm s.d. * $P < 0.05$, two-tailed Student's t -test. $n = 8$ mice per group (4 female and 4 male).



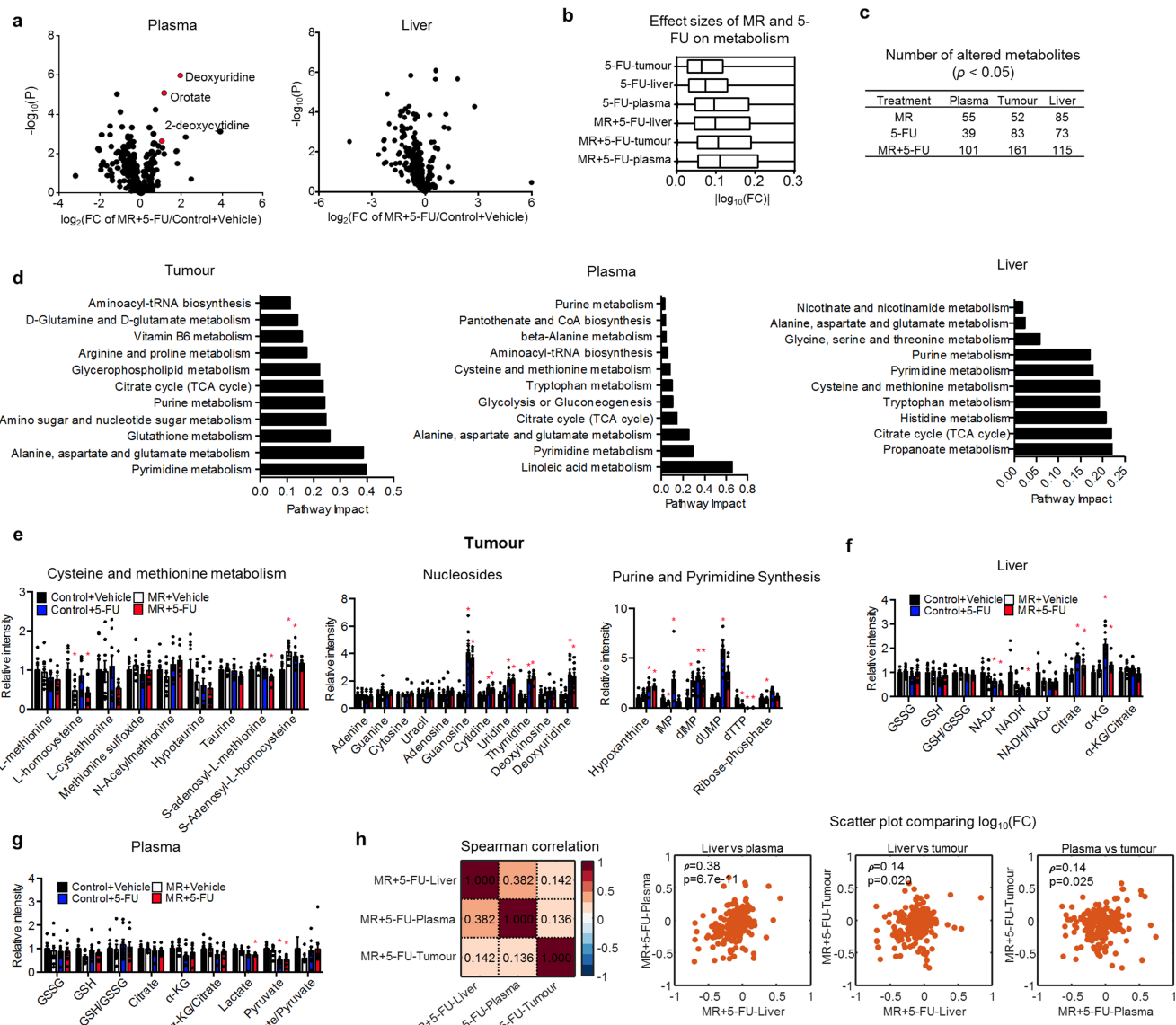
Extended Data Fig. 3 | Methionine restriction leads to specific cell-intrinsic metabolic alterations in tumours. To determine whether the effect of methionine restriction on tumour growth is systemic, cell autonomous or both, we conducted an integrated analysis of global changes in the metabolic network across tumour, plasma and liver within each model from the prevention study shown in Fig. 1f. $n = 8$ mice per group (4 female and 4 male). **a**, Spearman's rank correlation coefficients of fold change of metabolites in tumour, plasma and liver induced by methionine restriction exhibited strong correlations between each tissue pair, with the highest correlation between the tumour and the plasma in both CRC119 and CRC240. **b**, Multidimensional scaling analysis of metabolite fold change in response to methionine restriction. In both models, the fold change of metabolites in tumours showed a higher similarity with those in the plasma than with those in the liver. **c**, The effect of methionine restriction on metabolism in tumour, plasma and liver, evaluated by taking

the \log_{10} of the fold change. Box limits are the 25th and 75th percentiles, centre line is the median, and the whiskers are the minimal and maximal values. **d**, Numbers of metabolites significantly altered (* $P < 0.05$, two-tailed Student's t -test) by methionine restriction. $n = 8$ mice per group (4 female and 4 male). **e**, Schematic defining methionine-related metabolites (metabolized from or to methionine within four reaction steps) and methionine-unrelated metabolites. **f**, **g**, A higher proportion of altered metabolites was methionine-related in plasma and tumour compared to liver, in which metabolites altered by methionine restriction were nearly equally distributed between methionine-related and methionine-unrelated groups. **f**, Fraction of significantly (* $P < 0.05$, two-tailed Student's t -test) altered metabolites for methionine-related and methionine-unrelated metabolites in tumour, liver and plasma. **g**, Numbers of total and significantly altered metabolites for methionine-related and methionine-unrelated metabolites in tumour, liver and plasma. P values were determined by one-sided Fisher's exact test.



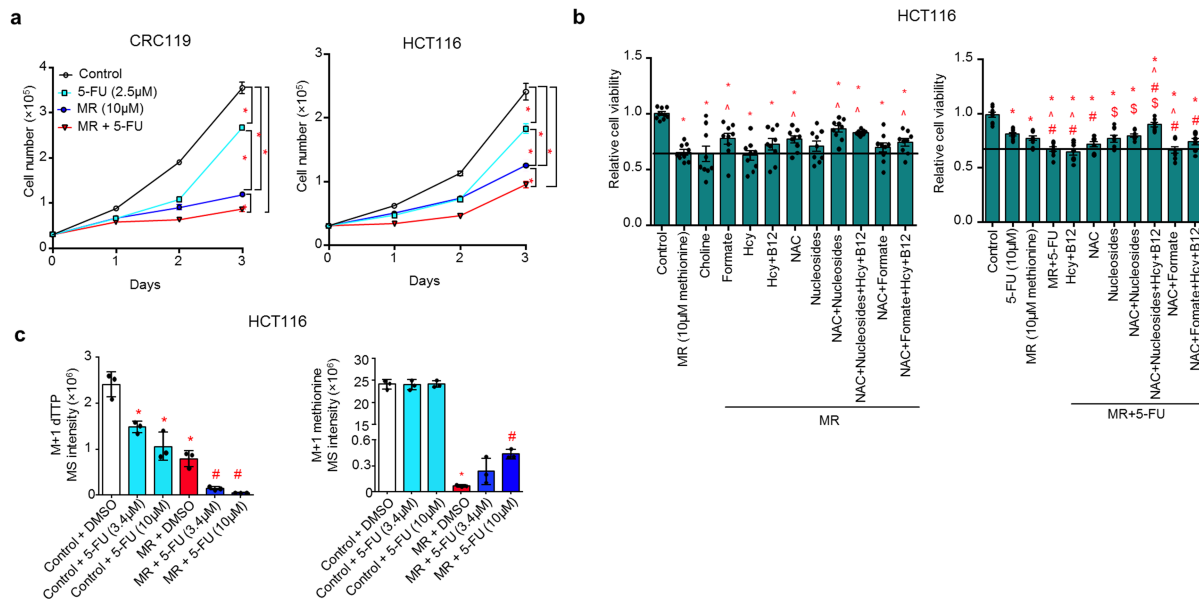
Extended Data Fig. 4 | Methionine restriction inhibits cell proliferation, and most substantially alters cysteine and methionine metabolism in primary colorectal cancer cells. **a**, Relative cell numbers in CRC119 and CRC240 primary tumour cells treated with different doses of methionine for 72 h. Mean \pm s.d. $n = 3$ biologically independent samples; similar results were obtained from 3 independent experiments. $*P < 0.05$, two-tailed Student's *t*-test. **b**, Volcano plots of metabolites in cells cultured in 0 or 100 μ M methionine for 24 h. *P* values were determined by two-tailed Student's *t*-test. **c**, Left, Venn diagram of significantly changed ($*P < 0.05$, two-tailed Student's *t*-test) metabolites in CRC119 and CRC240 primary

cells cultured with no methionine versus control (100 μ M methionine), and pathway analysis of metabolites that were commonly changed. Right, fold change of metabolites in cysteine and methionine metabolism, and pyrimidine metabolism, in CRC119 and CRC240 primary cells treated with 0 or 100 μ M methionine. Mean \pm s.d. $n = 3$ biologically independent samples. $*P < 0.05$, two-tailed Student's *t*-test. **d**, Relative fold change of intensity of amino acids by methionine deprivation in CRC119 and CRC240 primary cells. Mean \pm s.d. $n = 3$ biologically independent samples. $*P < 0.05$, two-tailed Student's *t*-test.



Extended Data Fig. 5 | Dietary restriction of methionine sensitizes PDX models of colorectal cancer to 5-FU chemotherapy. **a**, Volcano plots of metabolites in plasma and liver altered by the combination of dietary restriction of methionine and 5-FU treatment. P values were determined by two-tailed Student's t -test. **b**, Effect of 5-FU treatment alone, and a combination of methionine restriction and 5-FU treatment, on metabolites in tumour, plasma and liver, evaluated by taking the \log_{10} of the fold change. Box limits are the 25th and 75th percentiles, centre line is the median, and the whiskers are the minimal and maximal values. The data represents metabolites in liver (337), plasma (282) and tumour (332) from $n = 8$ mice per group. **c**, Numbers of metabolites significantly changed by methionine restriction, 5-FU treatment or the combination

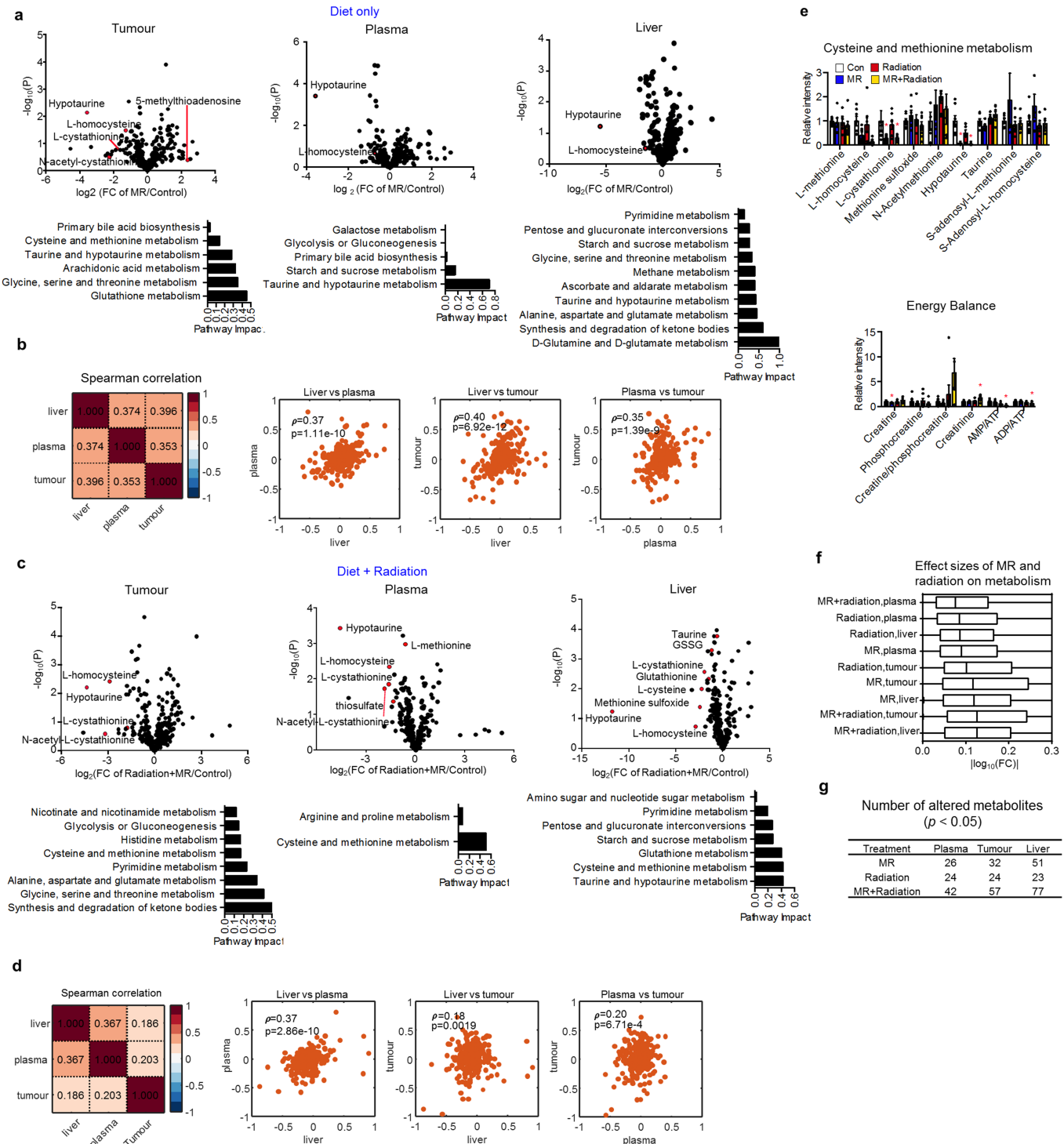
of methionine restriction and 5-FU treatment in plasma, tumour and liver. * $P < 0.05$, two-tailed Student's t -test. **d**, Pathway analysis of metabolites significantly changed (* $P < 0.05$, two-tailed Student's t -test) by methionine restriction, 5-FU treatment or the combination of dietary methionine restriction and 5-FU treatment (false discovery rate < 0.5). **e–g**, Relative intensity of metabolites related to cysteine and methionine metabolism, and nucleotide metabolism, in tumour (**e**) and redox balance in liver (**f**) and plasma (**g**). Mean \pm s.e.m. $n = 8$ mice per group. * $P < 0.05$, two-tailed Student's t -test. **h**, Spearman's rank correlation coefficients of methionine restriction and 5-FU-induced fold change of metabolites in tumour, plasma and liver from mice on dietary methionine restriction and with 5-FU treatment.



Extended Data Fig. 6 | Inhibition of cell growth mediated by methionine restriction is largely due to interruptions to the production of nucleosides and redox balance. **a**, The synergic effects of methionine restriction and 5-FU treatment in CRC119 primary cells and HCT116 cells were evaluated by cell counting. Mean \pm s.e.m. $n = 3$ biological replicates. * $P < 0.05$ by two-tailed Student's *t*-test. **b**, The rescue effect of choline, formate, homocysteine, homocysteine with vitamin B12, nucleosides and NAC, alone or in combination, on the inhibition of HCT116 cell proliferation mediated by methionine restriction. Mean \pm s.e.m., $n = 9$

biologically independent samples from 3 independent experiments.

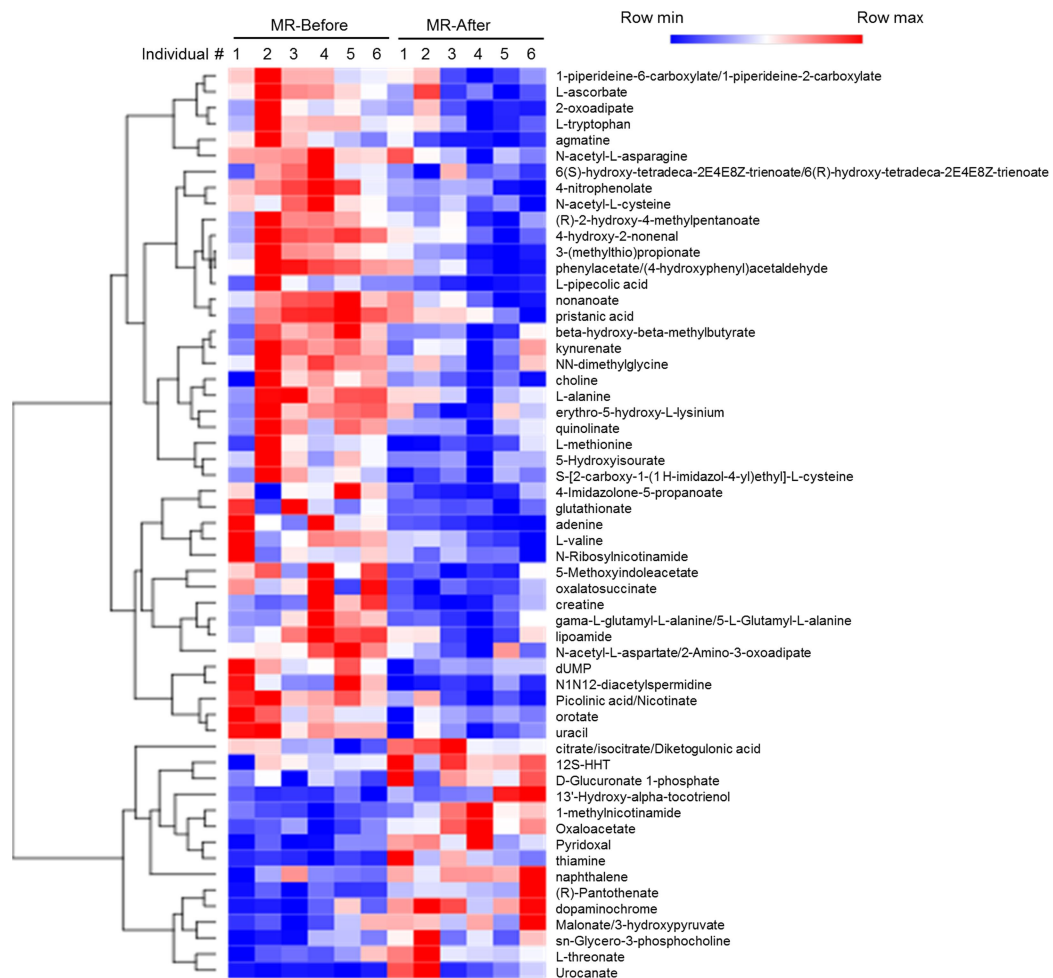
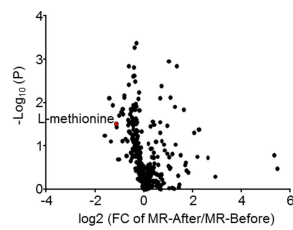
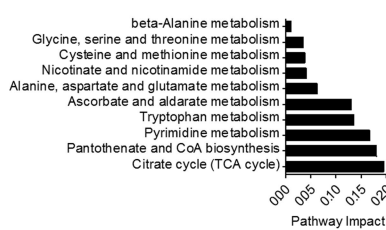
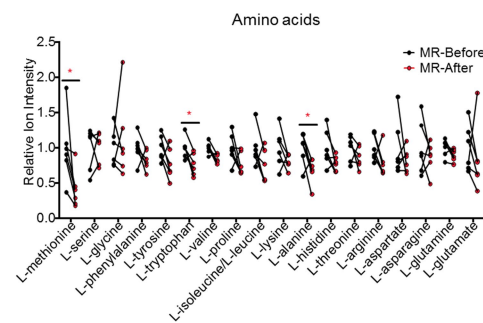
* $P < 0.05$ versus control, ^ $P < 0.05$ versus methionine restriction, # $P < 0.05$ versus 5-FU treatment, \$ $P < 0.05$ versus methionine restriction + 5-FU treatment, by two-tailed Student's *t*-test. **c**, Mass intensity for [M + 1] dTTP and [M + 1] methionine in HCT116 cells from the experiment described in Fig. 2h. Mean \pm s.d. $n = 3$ biologically independent samples. * $P < 0.05$ versus control and # $P < 0.05$ versus methionine restriction, by two-tailed Student's *t*-test.



Extended Data Fig. 7 | Dietary restriction of methionine sensitizes mouse models of RAS-driven autochthonous sarcoma to radiation.

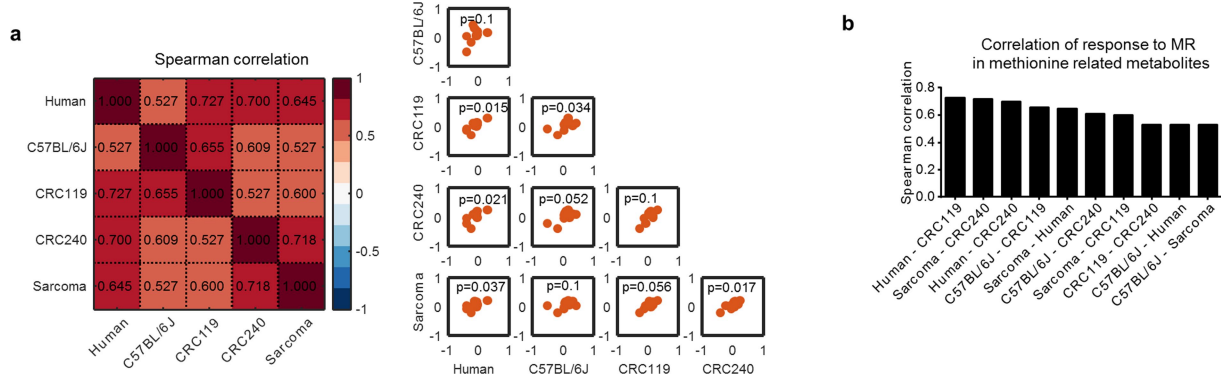
a, Volcano plots of metabolites in tumour, plasma and liver, and pathway analysis of metabolites significantly changed ($*P < 0.05$, two-tailed Student's t -test) by dietary restriction of methionine alone (false discovery rate < 1). **b**, Spearman's rank correlation coefficients of fold change of metabolites in tumour, plasma and liver induced by methionine restriction. **c**, Volcano plots of metabolites in tumour, plasma and liver, and pathway analysis of metabolites significantly changed ($*P < 0.05$, two-tailed Student's t -test) by dietary restriction of methionine and radiation (false discovery rate < 0.5). **d**, Spearman's rank correlation coefficients of fold change of metabolites in tumour, plasma and liver induced by methionine restriction and radiation. **e**, Relative intensity of

metabolites related to cysteine and methionine metabolism, and energy balance in tumours. Mean \pm s.d. $n = 7$ mice per group, except for the methionine-restriction group ($n = 6$). $*P < 0.05$ versus control, by two-tailed Student's t -test. **f**, **g**, The largest effects on metabolism occurred in the combination of diet and radiation. **f**, Effect of methionine restriction and radiation alone, or in combination, on metabolites in tumour, plasma and liver, evaluated by taking the \log_{10} of fold change. Box limits are the 25th and 75th percentiles, centre line is the median, and the whiskers are the minimal and maximal values. The data represent metabolites in liver (319), plasma (308) and tumour (332) from $n = 7$ mice per group, except for the methionine-restriction group ($n = 6$). **g**, Numbers of metabolites significantly changed ($*P < 0.05$, two-tailed Student's t -test) by methionine restriction and radiation alone, or in combination.

a**b****c****d**

Extended Data Fig. 8 | Dietary restriction of methionine can be achieved in humans. **a**, Heat map of significantly changed ($*P < 0.05$, two-tailed Student's t -test) plasma metabolites by dietary intervention, in six human subjects. **b**, Volcano plot of plasma metabolites. P values were

determined by two-tailed Student's t -test. **c**, Pathway analysis of altered ($*P < 0.05$, two-tailed Student's t -test) plasma metabolites. **d**, Relative intensity of amino acids in plasma. $n = 6$ biologically independent humans. $*P < 0.05$ by two-tailed Student's t -test.



Extended Data Fig. 9 | Comparative metabolic effects of methionine restriction across mouse models and humans. **a**, Spearman's rank correlation coefficients of fold changes of methionine-related metabolites induced by methionine restriction (defined in Extended Data Fig. 3f) in

plasma samples from non-tumour bearing C57BL/6J mice, CRC119 and CRC240 mouse models, the sarcoma mouse model and healthy human subjects. **b**, Spearman's rank correlation coefficients among different models in **a**, ranked from the highest to the lowest.

Extended Data Table 1 | Methionine concentrations in plasma, tumour and liver across mouse models and humans

Model	Tissue	Control diet	MR diet
CRC119	Plasma	37.58 ± 6.08	27.44 ± 4.28*
	Tumour	31.23 ± 9.10	20.08 ± 2.36*
	Liver	29.99 ± 2.38	18.68 ± 4.12*
CRC240	Plasma	52.35 ± 12.19	32.98 ± 3.60*
	Tumour	70.77 ± 25.73	31.82 ± 3.05*
	Liver	18.97 ± 3.10	12.393 ± 1.86*
CRC119 (Vehicle)	Plasma	35.93 ± 6.02	33.88 ± 7.97
	Tumour	33.52 ± 10.31	31.50 ± 12.12
	Liver	17.37 ± 4.18	16.68 ± 3.88
CRC119 (5-FU)	Plasma	32.13 ± 5.29	31.31 ± 11.55
	Tumour	26.70 ± 7.15	29.45 ± 11.04
	Liver	16.50 ± 5.14	16.61 ± 2.39
Sarcoma	Plasma	37.75 ± 5.27	35.86 ± 14.57
	Tumour	46.84 ± 10.01	38.39 ± 10.32
	Liver	10.44 ± 4.74	10.45 ± 3.44
Sarcoma (Radiation)	Plasma	24.44 ± 7.56	25.87 ± 4.11#
	Tumour	43.10 ± 11.86	37.22 ± 4.97#
	Liver	10.43 ± 2.98	6.55 ± 1.9*
C57BL/6J	Plasma	99.89 ± 16.90	28.79 ± 4.59*
Human	Plasma	13.74 ± 5.19	6.55 ± 4.02*

Tissues were collected at the end of each experiment. Concentrations in tissues were estimated in μM , assuming that 1 g wet tissue weight = 1 ml. Quantification was performed by using ^{13}C -labelled standards for each amino acid, which were added before extraction. Cyclic loess normalization and linear regression were applied in quantification of methionine in samples without ^{13}C -labelled standards. Values are mean ± s.d. $n = 8$ for CRC119, CRC240, CRC119 (vehicle) and CRC119 (5-FU), 7 for sarcoma on the control diet, 6 for sarcoma on the methionine-restricted diet, 7 for sarcoma (radiation), 5 for C57BL/6J mice and 6 for humans. * $P < 0.05$, by two tailed Student's *t*-test between the control diet and the methionine-restricted diet; # $P < 0.05$, by two tailed Student's *t*-test between the control diet and the methionine-restricted diet + radiation.

Reporting Summary

Nature Research wishes to improve the reproducibility of the work that we publish. This form provides structure for consistency and transparency in reporting. For further information on Nature Research policies, see [Authors & Referees](#) and the [Editorial Policy Checklist](#).

Statistics

For all statistical analyses, confirm that the following items are present in the figure legend, table legend, main text, or Methods section.

n/a Confirmed

- The exact sample size (n) for each experimental group/condition, given as a discrete number and unit of measurement
- A statement on whether measurements were taken from distinct samples or whether the same sample was measured repeatedly
- The statistical test(s) used AND whether they are one- or two-sided
Only common tests should be described solely by name; describe more complex techniques in the Methods section.
- A description of all covariates tested
- A description of any assumptions or corrections, such as tests of normality and adjustment for multiple comparisons
- A full description of the statistical parameters including central tendency (e.g. means) or other basic estimates (e.g. regression coefficient) AND variation (e.g. standard deviation) or associated estimates of uncertainty (e.g. confidence intervals)
- For null hypothesis testing, the test statistic (e.g. F , t , r) with confidence intervals, effect sizes, degrees of freedom and P value noted
Give P values as exact values whenever suitable.
- For Bayesian analysis, information on the choice of priors and Markov chain Monte Carlo settings
- For hierarchical and complex designs, identification of the appropriate level for tests and full reporting of outcomes
- Estimates of effect sizes (e.g. Cohen's d , Pearson's r), indicating how they were calculated

Our web collection on [statistics for biologists](#) contains articles on many of the points above.

Software and code

Policy information about [availability of computer code](#)

Data collection

No specific software was used for data collection.

Data analysis

Raw metabolomics data were processed with Sieve 2.0. from Thermo Scientific, Pathway analysis of metabolites was carried out with software Metaboanalyst (<http://www.metaboanalyst.ca/MetaboAnalyst/>) using the KEGG pathway database (<http://www.genome.jp/kegg/>). Cross-tissue comparison of metabolite profiles in PDX and sarcoma models were carried out in MATLAB R2018b. GraphPad PRISM 6.0 and Microsoft Excel were used for statistical analysis.

For manuscripts utilizing custom algorithms or software that are central to the research but not yet described in published literature, software must be made available to editors/reviewers. We strongly encourage code deposition in a community repository (e.g. GitHub). See the Nature Research [guidelines for submitting code & software](#) for further information.

Data

Policy information about [availability of data](#)

All manuscripts must include a [data availability statement](#). This statement should provide the following information, where applicable:

- Accession codes, unique identifiers, or web links for publicly available datasets
- A list of figures that have associated raw data
- A description of any restrictions on data availability

The metabolomics data reported in this study has been deposited to Mendeley Data (DOI: doi:10.17632/zs269d9fvb.1). Source code has been deposited to GitHub (https://github.com/LucasaleLab/Dietary_methionine_restriction). Source data are provided for all figures.

Field-specific reporting

Please select the one below that is the best fit for your research. If you are not sure, read the appropriate sections before making your selection.

Life sciences Behavioural & social sciences Ecological, evolutionary & environmental sciences

For a reference copy of the document with all sections, see nature.com/documents/nr-reporting-summary-flat.pdf

Life sciences study design

All studies must disclose on these points even when the disclosure is negative.

Sample size	Sample sizes were given in the manuscript. Efficacy studies in mice were conducted with 5 or more mice per group. No statistical methods were used to predetermine sample size.
Data exclusions	No data were excluded.
Replication	Replication numbers were reported in the text or in the methodology sections. Where appropriate a measure of the error was reported. All metabolic tracing and profiling, and cell counting study, were done once. For MTT assay, experiments were repeated at least three times with similar results. Biological replicates were produced.
Randomization	For all animal studies, mice were randomized into different research groups.
Blinding	For the dietary studies, the same investigators carried out the dietary treatment and downstream analysis, so were not blinded to group allocation.

Reporting for specific materials, systems and methods

We require information from authors about some types of materials, experimental systems and methods used in many studies. Here, indicate whether each material, system or method listed is relevant to your study. If you are not sure if a list item applies to your research, read the appropriate section before selecting a response.

Materials & experimental systems		Methods	
n/a	Involved in the study	n/a	Involved in the study
<input checked="" type="checkbox"/>	<input type="checkbox"/> Antibodies	<input checked="" type="checkbox"/>	<input type="checkbox"/> ChIP-seq
<input type="checkbox"/>	<input checked="" type="checkbox"/> Eukaryotic cell lines	<input checked="" type="checkbox"/>	<input type="checkbox"/> Flow cytometry
<input checked="" type="checkbox"/>	<input type="checkbox"/> Palaeontology	<input checked="" type="checkbox"/>	<input type="checkbox"/> MRI-based neuroimaging
<input type="checkbox"/>	<input checked="" type="checkbox"/> Animals and other organisms		
<input type="checkbox"/>	<input checked="" type="checkbox"/> Human research participants		
<input checked="" type="checkbox"/>	<input type="checkbox"/> Clinical data		

Eukaryotic cell lines

Policy information about [cell lines](#)

Cell line source(s)	CRC119 and CRC240 cell lines were developed from their respective CRC PDXs in Dr. David Hsu's lab at Duke University. HCT116 cell line was a gift from Dr. Lewis Cantley's laboratory.
Authentication	Cell lines were authenticated at the Duke University DNA Analysis Facility by analyzing DNA samples from each cell lines for polymorphic short tandem repeat (STR) markers using the GenePrint 10 kit from Promega (Madison, WI, USA).
Mycoplasma contamination	All cell lines were negative for mycoplasma contamination
Commonly misidentified lines (See ICLAC register)	No commonly misidentified cell lines were used.

Animals and other organisms

Policy information about [studies involving animals](#); [ARRIVE guidelines](#) recommended for reporting animal research

Laboratory animals	The following mouse strains were used in the manuscript: C57BL/6J mice: male, 12-week-old; NOD.CB17-PrkdcSCID-J mice: male and female, 8-10-week-old; NOD.Cg-Prkdcscid Il2rgtm1Wjl/SzJ mice: male and female, 8-10-week-old; C57BL/6J × 129SvJ mice carrying p53FRT and FSF-KrasG12D: male and female, 6-10-week-old;
--------------------	---

Wild animals

No wild animals were involved in this study.

Field-collected samples

The study did not involve samples collected from field.

Ethics oversight

All animal procedures and studies were approved by the Institutional Animal Care and Use Committee (IACUC) at Duke University. All animal experiments were performed in accordance with relevant guidelines and regulations.

Note that full information on the approval of the study protocol must also be provided in the manuscript.

Human research participants

Policy information about [studies involving human research participants](#)

Population characteristics

healthy human subjects (both male and female) recruited in the dietary study aged between 49-58 years old

Recruitment

Healthy adults of mixed gender were recruited by fliers and word of mouth and, as assessed for initial eligibility by telephone interview, were free of disease and currently not taking certain medications including anti-inflammatory drugs, corticosteroids, statins, thyroid drugs, and oral contraceptives. Final eligibility was assessed by standard clinical chemistry and hematology analyses. Written consent was obtained from eligible subjects. We are unaware of any potential self-selection bias or other biases present.

Ethics oversight

The controlled feeding study in healthy humans was conducted at Penn State University Clinical Research Center (CRC) and approved by the Institutional Review Board of the Penn State College of Medicine in accordance with the Helsinki Declaration of 1975 as revised in 1983 (IRB# 32378). We have complied with all relevant ethical regulations.

Note that full information on the approval of the study protocol must also be provided in the manuscript.